

## **Distribution Agreement**

In presenting this thesis as a partial fulfillment of the requirements for a degree from Emory University, I hereby grant to Emory University and its agents the non-exclusive license to archive, make accessible, and display my thesis in whole or in part in all forms of media, now or hereafter now, including display on the World Wide Web. I understand that I may select some access restrictions as part of the online submission of this thesis. I retain all ownership rights to the copyright of the thesis. I also retain the right to use in future works (such as articles or books) all or part of this thesis.

Emilie C. Ung

April 10, 2023

*In Vitro* Expansion of Murine  $\gamma\delta$  T Cells and Transfection of Human  $\gamma\delta$  T cells for CAR T Cell  
Therapy

by

Emilie C. Ung

Dr. H. Trent Spencer  
Adviser

Biology

Dr. H. Trent Spencer  
Adviser

Dr. Skye Comstra  
Committee Member

Dr. Haydn T. Kissick  
Committee Member

2023

*In Vitro* Expansion of Murine  $\gamma\delta$  T Cells and Transfection of Human  $\gamma\delta$  T cells for CAR T Cell  
Therapy

By

Emilie C. Ung

Dr. H. Trent Spencer

Adviser

An abstract of  
a thesis submitted to the Faculty of Emory College of Arts and Sciences  
of Emory University in partial fulfillment  
of the requirements of the degree of  
Bachelor of Science with Honors

Biology

2023

## Abstract

### *In Vitro* Expansion of Murine $\gamma\delta$ T Cells and Transfection of Human $\gamma\delta$ T cells for CAR T Cell Therapy

By Emilie C. Ung

CAR T cell therapy has emerged as one of the most promising ways to treat cancer and is currently being studied as a potential treatment for AML (Leick et al. 2022). In particular,  $\gamma\delta$  T cells have special promise due to their ability to kill cancer in an off-the-shelf manner without inducing graft-versus-host-disease (GVHD). We want to develop a syngeneic mouse model to study whether murine  $\gamma\delta$  T cells from the bone marrow preferentially home to the bone marrow. Our study focused on developing a protocol for expanding murine  $\gamma\delta$  T cells. In this study, we tested the ability of CD3/CD28 beads, zoledronate, lipopolysaccharides (LPS), and Concanavalin A (ConA) to activate murine  $\gamma\delta$  T cells. Our findings have shown that of our tested activators, ConA provides the greatest percentage of murine  $\gamma\delta$  T cells, but is lacking in its expansion ability. We have also found that when using ConA, by the end of the expansion, there is a greater number of murine  $\gamma\delta$  T cells from the spleen rather than from the bone marrow. In addition, we optimized a protocol for transfecting human  $\gamma\delta$  T cells with an SCF-CAR through electroporation. This was done by collecting blood samples from human donors and isolating the PBMCs, performing an  $\alpha\beta$  T cell depletion on day 6, and cryopreserving them on day 14. When required for experiments, they were thawed and electroporated. The next day, flow cytometry analysis was done to determine the success of the electroporation conditions, where we found the Biorad 4 mm cuvettes electroporated for 2 ms at 500 volts were considered to be the optimal condition. This work has the ability to provide tools that will help us learn more about the biology of murine and human  $\gamma\delta$  T cells.

*In Vitro* Expansion of Murine  $\gamma\delta$  T Cells and Transfection of Human  $\gamma\delta$  T cells for CAR T Cell  
Therapy

By

Emilie C. Ung

Dr. H. Trent Spencer

Adviser

A thesis submitted to the Faculty of Emory College of Arts and Sciences  
of Emory University in partial fulfillment  
of the requirements of the degree of  
Bachelor of Science with Honors

Biology

2023

## Acknowledgments

I would like to thank:

The Spencer-Doering Lab for supporting me throughout this process! From your kind welcomes on my first day to answering my many questions during my experiments, I feel extremely lucky to not only have found a lab that works on ground-breaking research but also has some fantastic people.

Dr. Spencer, thank you for taking a chance on an undergraduate who had nothing to her name except a passion for biotechnology. While this process has not been easy, I am sincerely grateful for the growth I have made as a scientist due to your guidance.

Gianna, thank you for letting me shadow you for these past few years. I will be forever grateful for your unwavering patience, your kind words, and your gift of teaching that I have benefited from. I'm wishing the best of luck for your surely bright future ahead!

Dr. Comstra and Dr. Kissick, for your advice throughout this process!

Thank you!

## Table of Contents

Introduction	1
Methods	6
Results	18
Discussion	23
References	27

### **Tables and Figures**

Figure 1	31
Figure 2	32
Figure 3	33
Figure 4	34
Figure 5	35
Figure 6	36
Table 1	37
Figure 7	38
Figure 8	39
Figure 9	40
Figure 10	41
Figure 11	42
Figure 12	43
Figure 13	44
Figure 14	45
Figure 15	46

Figure 16	47
Figure 17	48
Figure 18	49
Figure 19	50
Figure 20	51
Figure 21	52
Figure 22	53
Table 2	54
Figure 23	55



## Abstract

### *In Vitro* Expansion of Murine $\gamma\delta$ T Cells and Transfection of Human $\gamma\delta$ T cells for CAR T Cell Therapy By Emilie C. Ung

CAR T cell therapy has emerged as one of the most promising ways to treat cancer and is currently being studied as a potential treatment for AML (Leick et al. 2022). In particular,  $\gamma\delta$  T cells have special promise due to their ability to kill cancer in an off-the-shelf manner without inducing graft-versus-host-disease (GVHD). We want to develop a syngeneic mouse model to study whether murine  $\gamma\delta$  T cells from the bone marrow preferentially home to the bone marrow. Our study focused on developing a protocol for expanding murine  $\gamma\delta$  T cells. In this study, we tested the ability of CD3/CD28 beads, zoledronate, lipopolysaccharides (LPS), and Concanavalin A (ConA) to activate murine  $\gamma\delta$  T cells. Our findings have shown that of our tested activators, ConA provides the greatest percentage of murine  $\gamma\delta$  T cells, but is lacking in its expansion ability. We have also found that when using ConA, by the end of the expansion, there is a greater number of murine  $\gamma\delta$  T cells from the spleen rather than from the bone marrow. In addition, we optimized a protocol for transfecting human  $\gamma\delta$  T cells with an SCF-CAR through electroporation. This was done by collecting blood samples from human donors and isolating the PBMCs, performing an  $\alpha\beta$  T cell depletion on day 6, and cryopreserving them on day 14. When required for experiments, they were thawed and electroporated. The next day, flow cytometry analysis was done to determine the success of the electroporation conditions, where we found the Biorad 4 mm cuvettes electroporated for 2 ms at 500 volts were considered to be the optimal condition. This work has the ability to provide tools that will help us learn more about the biology of murine and human  $\gamma\delta$  T cells.

# Introduction

Acute myeloid leukemia (AML) is a cancer of hematopoietic (blood) cells within the myeloid compartment (Döhner, Weisdorf, and Bloomfield 2015). Although there is an 80-90% survival rate for AML in childhood, a recurrence of AML results in a drop to a 21-33% likelihood of survival, emphasizing a need for novel therapeutics (Rubnitz et al. 2007).

Chimeric Antigen Receptor (CAR) T cell therapy has emerged as one of the most promising ways to treat cancer. In particular, there has been success in directing CD19 CAR T cell therapy toward B cell cancers (Razavi et al. 2023), even going so far as to achieve long-duration remission toward B cell lymphoma (Kochenderfer et al. 2017). CAR T cell therapy is currently being studied as a potential treatment for AML (Leick et al. 2022). CAR T cell therapy is unique because it does not require the use of the major histocompatibility complex (MHC) to present an antigen to a T cell (Gross, Waks, and Eshhar 1989). Instead, T cells can be modified to express the CAR (Branella and Spencer 2021) with a plasmid via electroporation or with a lentiviral vector (Gill, Maus, and Porter 2016). The purpose of a CAR is to redirect the T cells' killing capabilities toward a specific cell of choice. CARs are modular proteins that contain the main activation domain (CD3 $\zeta$ ) and costimulatory domains required for T cell activation. Their antigen specificity is derived from the combination of the variable heavy and variable light chains of an antibody, otherwise known as a single-chain variable fragment (scFv), or a naturally expressed receptor or ligand. In ligand-based CAR T cell therapy, the ligand of the modified T cell will bind to the cancer cell and lead to apoptosis of the cancer cell (Branella and Spencer 2021). In the case of CD19-directed therapeutics, the CD19 CAR will bind to the CD19 receptor on B cell acute lymphoid leukemia (B-ALL) (Salter, Pont, and Riddell 2018). Because hematopoietic cells originate from the bone marrow (Jagannathan-Bogdan and Zon 2013), and

myeloid depletion cannot be managed like B cell aplasia with CD19-directed CAR T therapy, bone marrow hematopoietic stem cells are one of the expected on-target, off-tumor toxicities for the treatment of AML (Mardiana and Gill 2020). Thus, the use of CAR T therapy in this setting can also be used as a bridge-to-transplant therapeutic as a non-genotoxic pre-conditioning regimen (Branella and Spencer 2021).

Specifically, our lab works with a ligand-based CAR whose ligand is stem cell factor (SCF), known as an SCF-CAR (Figure 2). SCF is a protein that binds to a c-kit receptor (Zsebo et al. 1990). This receptor is a target for AML because 60-80% of AML patients express c-kit on their myeloblasts. Furthermore, this receptor is a receptor tyrosine kinase (RTK), and of the RTK mutations, 17% of those are mutations in c-kit (Malaise, Steinbach, and Corbacioglu 2009). This allows our SCF-CAR to bind to cancerous myeloblasts, and therefore provide treatment for AML.

In particular, gamma delta ( $\gamma\delta$ ) T cells have shown great promise for CAR T cell therapy. While they are only composed of 1-10% of the peripheral blood population,  $\gamma\delta$  T cells have a natural ability to kill cancer without the need for the MHC complex (Jhita and Raikar 2022). This concept works hand in hand with CAR T cell therapy. This is especially crucial since the MHC complex is one of the determinants of whether an organism will have a negative immunological response to a transplanted organ, also known as graft-versus-host disease (GVHD) (Petersdorf 2013). This has implications for the ability to use  $\gamma\delta$  T cells “off the shelf” (Jhita and Raikar 2022) rather than having to personalize treatments to HLA-match (Torikai and Cooper 2016).

There have been great strides made in the progress of understanding human  $\gamma\delta$  T cells. For example, we have developed a protocol to expand human  $\gamma\delta$  T cells from peripheral blood

nuclear cells (PBMCs) (Jhita and Raikar 2022; Sutton et al. 2016) and studied characteristics that can determine who will significantly expand their numbers of  $\gamma\delta$  T cells (Burnham et al. 2020). However, our understanding of mouse (murine)  $\gamma\delta$  T cells is lacking in comparison due to difficulties in isolating and expanding  $\gamma\delta$  T cells (Williams et al. 2022). This difficulty is due in part to different genotypes of  $\gamma\delta$  T cells in mice and humans. In humans, the  $\gamma\delta$  T cell subset V $\gamma$ 9 $\delta$ 2 is expanded because of its cytotoxicity toward cancer cells (Saura-Esteller et al. 2022) and because it is simpler to expand subset V $\delta$ 2 from the blood (Burnham et al. 2020), where it is predominantly found (Saura-Esteller et al. 2022). In mice, it is more common to find  $\gamma\delta$  T cells in the mucosal tissues. Furthermore,  $\gamma\delta$  T cells are instead divided by V $\gamma$  subsets where the V $\gamma$ 1 subtype is harvested from the spleen and bone marrow (Qu et al. 2022). Specifically, the expansion of murine  $\gamma\delta$  T cells from the bone marrow would be preferred in order to determine how murine  $\gamma\delta$  T cells traffic to the bone marrow. However, we will also attempt to expand murine  $\gamma\delta$  T cells from other organs in order to gather greater numbers of  $\gamma\delta$  T cells, such as the spleen.

While this study focuses on  $\gamma\delta$  T cells for the SCF-CAR, the other T cell subtype is the  $\alpha\beta$  T cell. While all T cells contain a CD3 receptor,  $\gamma\delta$  T cells are differentiated by both their antigen binding sequences (Morath and Schamel 2020) and their  $\gamma\delta$  T cell receptor (TCR) (Figure 1) while  $\alpha\beta$  T cells contain an  $\alpha\beta$  TCR (Morath and Schamel 2020). The challenge of  $\alpha\beta$  CAR T cell therapy is that  $\alpha\beta$  T cells must be matched to their donor to reduce the risk of GVHD, and therefore autologous CAR T cells are preferred. However, it is occasionally unfeasible to retrieve autologous  $\alpha\beta$  CAR T cells from the cancer patient. To solve this issue, one research group used genome editing to remove the  $\alpha\beta$  TCR from healthy donors' T cells, creating an "off-the-shelf" CAR T cell product for refractory or relapsed B cell acute

lymphoblastic lymphoma (Benjamin et al. 2020) that has completed Phase 1 clinical trials (Benjamin et al. 2022). For our experiments, the  $\alpha\beta$  T cells must be removed in order to ensure a purified sample of  $\gamma\delta$  T cells.

The purpose of a murine  $\gamma\delta$  T cell model would be to create a syngeneic mouse model that will be used to account for the limitations of using an NSG mouse model. CAR T cell therapy is often modeled in mice using human cancers in murine models. Humanized mouse models may better recapitulate the human immune system, but they are still incomplete (Tassone et al. 2012) and cost-prohibitive (Richards et al. 2020). Our current model limits our ability to study  $\gamma\delta$  interactions with the host immune system, which would be relevant in clinical trials, especially when considering toxicity. In our lab, we have been unable to see human  $\gamma\delta$  T cells migrate into murine bone marrow. As a result, we are interested to see if murine  $\gamma\delta$  T cells have a location they would prefer to migrate to.

In addition to looking at murine  $\gamma\delta$  T cells, we wanted to optimize the protocol for transfecting the SCF-CAR into human  $\gamma\delta$  T cells. While there are optimized protocols available for  $\alpha\beta$  T cells provided by the manufacturer, we do not have any for  $\gamma\delta$  T cells. This will be important in order to ensure that our SCF-CARs are both viable and express the CAR, both of which are indicators of a good quality product.

We tested the CD3/CD28 beads, zoledronate, LPS, and ConA for their ability to activate murine  $\gamma\delta$  T cells for expansion. We chose CD3/CD28 beads as it has been seen that these materials have been shown to produce 150-fold murine  $\gamma\delta$  T cell expansion (Williams et al. 2022). Zoledronate was used as it is able to expand human  $\gamma\delta$  T cells by inhibiting the mevalonate pathway, causing isopentenyl pyrophosphate (IPP) to accumulate and activate V $\delta$ 2 T cells (Chiarella et al. 2020). Our lab has used zoledronate successfully to produce a mean of

80-fold expansion with human  $\gamma\delta$  T cell expansions (Sutton et al. 2016). In addition, LPS has been shown to interact with murine  $\gamma\delta$  T cells through toll-like receptor 4 (Tlr4) (Poltorak et al. 1998). Lastly, we have seen that ConA has been used to expand both human  $\gamma\delta$  T cells (Siegers et al. 2011) and murine T cells (Rafiq et al. 2018), and wanted to test whether it could selectively isolate  $\gamma\delta$  T cells in mice.

We hypothesize that murine  $\gamma\delta$  T cells will expand by activating female spleens with zoledronate. Some of the factors that will need to be considered include the organs that  $\gamma\delta$  T cells reside in most, the gender of the mouse that provides the greatest product of  $\gamma\delta$  T cells, ensuring an effective  $\alpha\beta$  T cell depletion, and providing the correct activator for  $\gamma\delta$  T cells while ensuring that  $\alpha\beta$  T cells do not expand. The goal is to determine whether murine  $\gamma\delta$  T cells will home to the bone marrow and if murine  $\gamma\delta$  T cells will home to the spleen. This, combined with the transfection studies on human  $\gamma\delta$  T cells, are designed to learn more about the biology of  $\gamma\delta$  T cells.

## Methods

### *Murine $\gamma\delta$ T cell Expansion Protocol*

#### **Murine Spleen Isolation**

A male or female 4-8 week old Balb/C or Bl/6 mouse was euthanized and the spleen was harvested. The spleens were placed into an Eppendorf tube with 1 mL of sterile phosphate-buffered saline (PBS) and stored on ice until they were ready to be crushed. Spleens were separated into Eppendorf tubes by sex. Within a sterile cell culture hood, for each Eppendorf tube, a 40  $\mu$ M cell strainer was placed on top of a 50 mL conical tube and pre-wet with 1 mL of sterile PBS before the sterile PBS was discarded. The contents of the Eppendorf tube (containing spleens and 1 mL of PBS) were mashed with the end of a 1.5 mL syringe. Then the end of the 1.5 mL syringe and the cell strainer was washed twice with 2 mL of sterile PBS.

#### **Murine Bone Marrow Isolation**

A male or female 4-8 week old Balb/C or CD45.1 Bl/6 mouse was euthanized and the femurs and tibias from both legs were harvested. All bones were dipped into ethanol before being placed into an Eppendorf tube with 1 mL of sterile PBS and stored on ice until they were ready to be flushed. Bones were separated into Eppendorf tubes by sex. Within a sterile cell culture hood, both ends of the tibia and femurs were cut off. Tibias were flushed with a 23G needle using 1 mL of sterile PBS until completely clear. Femurs were flushed with a 26G  $\frac{5}{8}$  needle using 1 mL of sterile PBS until completely clear. Once the bones were flushed, each tube of bone marrow cells (separated by sex) was resuspended. For each Eppendorf tube, a 40  $\mu$ M cell strainer was placed on top of a 50 mL conical tube and pre-wet with 1 mL of sterile PBS before the sterile PBS was

discarded. The contents of the Eppendorf tube (containing bone marrow cells) were transferred to the cell strainer and washed twice with 2 mL of sterile PBS.

### **Murine $\gamma\delta$ T Cell Culture**

On Day 0, any samples from the bone marrow and/or the spleen (separated by organ and by sex) were centrifuged at 4°C and 300 g for 10 minutes. Once the supernatant was removed, the cells were resuspended in 3 mL of Red Blood Cell (RBC) Lysis Buffer and left to sit at room temperature for 10 minutes before they were centrifuged at 4°C and 300 g for 10 minutes. During this time, cells were counted. After the supernatant was removed, the cells were resuspended in complete murine  $\gamma\delta$  T cell media at a concentration of  $5 \times 10^6$  live cells/mL and 500 IU/mL of interleukin-2 (IL-2). This culture was activated with either 1  $\mu$ g LPS per mL of murine  $\gamma\delta$  T cell media, 4  $\mu$ g of ConA per mL of murine  $\gamma\delta$  T cells media, 1.67  $\mu$ L of zoledronate per mL of murine  $\gamma\delta$  T cells media, or CD3/CD28 beads at a concentration of 25  $\mu$ L of beads per  $10^6$  cells. This culture was incubated at 37°C and 5% CO<sub>2</sub> when actively being re-cultured. Reculturing occurred on Day 3, Day 5, and Day 7 (Figure 3). On these days, the cells were cultured in complete murine  $\gamma\delta$  T cell media at a concentration of  $3 \times 10^6$  live cells/mL and 1000 IU/mL of IL-2.

### **Murine $\gamma\delta$ T Cell Media**

Murine  $\gamma\delta$  T cell media is made of 10% Fetal Bovine Serum (FBS), 1% Penicillin-Streptomycin (Pen-Strep) (10,000 units penicillin and 10 mg streptomycin/mL), and 3% All The Other Stuff (ATOS) in Roswell Park Memorial Institute (RPMI). ATOS consists of equal volumes of 1M N-2-hydroxyethylpiperazine-N'-2-ethanesulfonic acid (1M HEPES Buffer), 100 mM sodium



pyruvate, and 100X Minimum Essential Medium (MEM) Non-Essential Amino Acids (NEAA). Also included in ATOS is 8  $\mu\text{L}$  of 2-mercaptoethanol ( $\beta\text{-ME}$ ) for every 13 mL of ATOS.

### **Bead Activation/Removal**

On day 0 or day 3, CD3 and CD28 Dynabeads were used for murine  $\gamma\delta$  T cell activation. The beads were vortexed for 30 seconds before they were transferred into a 1.5 mL Eppendorf tube at a concentration of 6.25  $\mu\text{L}$  or 25  $\mu\text{L}$  of beads per  $10^6$  cells along with 1 mL of complete murine  $\gamma\delta$  T cell media and 100 or 500 IU/mL of IL-2. Each Eppendorf tube contained a different experimental condition. The Eppendorf tube was then placed on a magnet for one minute before all the complete  $\gamma\delta$  T cell media was removed. Then the Eppendorf tube was removed from the magnet and the beads were resuspended in 1 mL of complete murine  $\gamma\delta$  T cell media and 100 IU or 500 IU of IL-2. The contents of the tube were resuspended into the appropriate cell culture plate or flask.

In order to remove the beads on day 3 (if they were added on day 0) or on day 5 (if they were added on day 3), the cells were resuspended before being inserted into Eppendorf tubes. The cell culture plate was washed with 1 mL of complete  $\gamma\delta$  T cell media before the tubes were placed on a magnet for one minute. After this, the cells were retrieved from the Eppendorf tube and the beads were discarded.

### **Zoledronate Activation**

On Day 0, zoledronate was resuspended in murine  $\gamma\delta$  T cell culture at a concentration of 1.67  $\mu\text{L}/\text{mL}$ .

## **LPS Activation**

On Day 0 or Day 3, LPS was resuspended in complete murine  $\gamma\delta$  T cell media at a concentration of 1  $\mu\text{g}/\text{mL}$ .

## **ConA Activation**

On Day 0 or Day 3, ConA was resuspended in murine  $\gamma\delta$  T cell culture at a concentration of 4  $\mu\text{g}/\text{mL}$  of murine  $\gamma\delta$  T cell media.

## **Negative Selection**

On Day 0 or Day 3, the murine  $\gamma\delta$  T cells underwent a negative selection for murine  $\gamma\delta$  T cells. First, cells were collected and counted as a pre-column control sample for flow cytometry. Next, cells were spun at 4°C and 300 g for 10 minutes. Once the cells were completely free of supernatant (a P1000 pipet was used to remove any excess liquid after dumping the supernatant), they were resuspended in  $1 \times 10^8$  cells/mL of isolation buffer (PBS + 5% sterile FBS). For each experimental group, either a combination of Biotin anti-CD11b, anti-B220, anti-CD4, and anti-CD8 antibodies, a pairing of Biotin anti-CD4 and Biotin anti-CD8 beads, or only Biotin anti-TCR $\beta$  antibodies were resuspended at a concentration of 0.1 or 10  $\mu\text{L}/\text{mL}$  before they were incubated at 4°C for 20 minutes. Then up to 10 mL of isolation buffer was added to each experimental group before they were centrifuged at 4°C and 300 g for 10 minutes. After the supernatant was completely discarded, cells were resuspended in  $1 \times 10^8$  cells/mL of isolation buffer and 20  $\mu\text{L}$  of anti-Biotin microbeads or anti-PE beads per  $10^7$  cells. Then the cells were

incubated at 4°C for 15 minutes before up to 10 mL of isolation buffer was added and the cells were centrifuged at 4°C and 300 g for 10 minutes.

While the cells were spinning, the magnetic LD or LS separation column was pre-wet with 3 mL of isolation buffer and the effluent was discarded from the collection tube. Once the cells finished spinning, the supernatant was removed until the cell pellet was completely dry before resuspending the cell pellet (up to  $1 \times 10^8$  cells) in 3 mL of isolation buffer. The cells were added to the LD or LS column and then washed 3 times with 3 mL of isolation buffer. Using a new tube, a sample from the column was collected by adding 3 mL of isolation buffer and retrieving the cells from the column by pushing with the provided plunger. From here, a 100  $\mu$ L sample from the column was taken for flow cytometry and the post-column sample (with the  $\gamma\delta$  T cells) was cultured before the sample was analyzed with flow cytometry.

## **Flow Cytometry**

Cells were counted in order to retrieve 100,000 cells for staining per flow tube sample, with the exception of the live/dead controls containing 50,000 live cells and 50,000 dead cells. The controls included obtaining one drop of unstained compensation beads, 1  $\mu$ L of murine  $\gamma\delta$  TCR stained with one drop of compensation beads, 1  $\mu$ L of murine CD3 stained with one drop of compensation beads, unstained cells, live and dead cells stained with 5  $\mu$ L of 1:1000 diluted eFluor 780, and a sample of cells from each experimental group containing our full stain, which was comprised of 3  $\mu$ L of murine  $\gamma\delta$  TCR and CD3, and 5  $\mu$ L of diluted eFluor 780 per sample.

When undergoing the staining protocol, 2 mL of FACS buffer (PBS + 2.5% FBS) was added to each flow tube sample containing cells and spun down at 4°C and 320 g for 3 minutes. Once the supernatants were discarded, the dead tube was placed on a 100°C heat block for 3 minutes, then cooled at 4°C (on ice) for 3 minutes before being combined with the dead tube. In addition to the stain, each tube containing compensation beads also had 100 µL of FACS buffer. The beads and the appropriate amount of stain were added to each tube sample. Each tube was vortexed before incubation at 4°C on ice for 10 minutes. Then the tubes were vortexed once again and incubated at 4°C for another 10 minutes. In some cases where the ice method was not preferred, the samples were incubated at room temperature for a total of 10 minutes and vortexed right before incubation and 5 minutes after incubation. Once incubation was complete, all the flow tube samples were given 2 mL of FACS buffer and then spun at 4°C and 320 g for 3 minutes. Once the supernatant was dumped, the cells were either immediately analyzed with flow cytometry or stored at 4°C until the time of flow cytometry.

The cytometer was programmed to collect at most 5,000 live events for compensation and 20,000 live events per experimental sample.

### *Human $\gamma\delta$ T cell Electroporation Protocol*

#### **Isolating Human $\gamma\delta$ T cells from Blood**

On day 0, PBMCs from human donors was collected at a volume between 10-20 mL. The criteria of these donors included non-smokers with a BMI between 20-25 and between the ages of 18-30 years old. After removing blood from the collection tubes and into 50 mL conical tubes, the volume of blood was recorded and 2 mL of PBS was used to wash the collection tube. After

resuspending the blood, 8 mL of blood were aliquoted into 15 mL tubes that already contained 5 mL of Ficoll-Paque density gradient media that had been warmed to 18°C to 20°C. These conicals were centrifuged at 20°C and 2000 rpm for 30 minutes. An eye-dropper was used to collect the mononuclear cell layer (second from the top), which contained our  $\gamma\delta$  T cells. The rest was discarded. The  $\gamma\delta$  T cells were resuspended in 6 mL of PBS and then centrifuged at 20°C and 2000 rpm for 10 minutes. After, 10 mL of OpTmizer media was added and the samples were centrifuged at 20°C and 2000 rpm for 10 minutes before the supernatant was discarded. Cells were resuspended in 10 mL of OpTmizer and counted. When culturing in  $\gamma\delta$  T cell media and IL-2 on Day 0, OpTmizer was not removed.

### **Human $\gamma\delta$ T Cell Activation and Culture**

On day 0, in addition to the 10 mL of OpTmizer media already present, cells were resuspended in complete human  $\gamma\delta$  T cell media at a concentration of  $1.5 \times 10^6$  cells/mL, IL-2 at a concentration of 500 IU/mL of complete  $\gamma\delta$  T cell media, and activated with 5 mM of zoledronate (50  $\mu$ L per 30 mL of media). On day 3, the  $\gamma\delta$  T cells were resuspended in complete  $\gamma\delta$  T cell media at a concentration of  $1.5 \times 10^6$  cells/mL with 500 IU/mL of IL-2 and activated with 5 mM of zoledronate. On days 6, 9, and 12,  $\gamma\delta$  T cells were resuspended at a concentration of  $1.5 \times 10^6$  cells/mL along with 1000 IU/mL of IL-2.

### **Human $\gamma\delta$ T Cell Media**

The human  $\gamma\delta$  T cells were suspended in 1 L of OpTmizer media supplemented with 26 mL of OpTmizer supplement, 10 mL of 200 mM L-glutamine, and 10–50  $\mu$ g/mL of Pen-Strep.

## Human $\alpha\beta$ T cell Depletion

On day 6, cells were counted and then centrifuged at 300 g for 5 minutes. Cells were re-counted in sterile PBS at a concentration of  $1 \times 10^6$  cells/mL and 300-500  $\mu$ L were removed to be used as a pre-column sample for flow cytometry. The cells were centrifuged at 250 g for 10 minutes and the supernatant was discarded before the cells were resuspended in  $\alpha\beta$  depletion buffer (7.5% BSA (in PBS) was added to create a 5% BSA solution in autoMACS rinsing solution) at a concentration of 98  $\mu$ L/ $10^6$  cells. Then 2 mL of anti- $\alpha\beta$  TCR-Biotin antibody was added per 98  $\mu$ L of buffer and incubated at 4°C for 10 minutes in a dark room. Cells were washed with 1-2 mL of depletion buffer and centrifuged for 10 minutes. The supernatant was resuspended in 80 $\mu$ L of depletion buffer for every  $10^7$  cells.

A 30  $\mu$ M cell strainer was pre-wet with depletion buffer and the buffer that passed through the collection tube was discarded before the cells were added to the strainer. The strainer was washed with 1-2 mL of depletion buffer. Then 20  $\mu$ L of anti-biotin microbeads per  $10^7$  cells were resuspended into the cells and incubated at 4°C for 15 minutes. The cells were washed with 1-2 mL of  $\alpha\beta$  depletion buffer per 10 million cells and spun for 10 minutes before the supernatant was discarded and resuspended up to  $10^8$  cells in 500  $\mu$ L of depletion buffer.

Next, an LD column was prepared by pre-wetting the column with 2 mL of depletion buffer and discarding the buffer in the collection tube before adding the cells to the column. Once the cells were added, the column was washed 3 times with 3 mL of depletion buffer. These cells are to be cultured as the post-column sample of  $\gamma\delta$  T cells. The cells bound to the column were collected by washing the column with 3 mL of depletion buffer and pushing the cells through with the

plunger. These cells were diluted with up to 5-7 mL of PBS and 300-500  $\mu\text{L}$  was collected for flow as the column sample. The post-column sample of  $\gamma\delta$  T cells was centrifuged for 10 minutes and resuspended in OpTmizer complete media or RPMI at a concentration at the previously stated concentration of  $1.5 \times 10^6$  cells/mL and 1000 IU/mL of IL-2.

## Flow Cytometry

On day 0, 1 mL of cells, but on days 6, 9, and 12, 500  $\mu\text{L}$  of the cell culture was retrieved for staining for each flow tube sample, with the exception of the live/dead control containing 300  $\mu\text{L}$  of live cells and 300  $\mu\text{L}$  of dead cells. The controls included obtaining one drop of unstained compensation beads, 2  $\mu\text{L}$  of  $\gamma\delta$  TCR stained with one drop of compensation beads, 1  $\mu\text{L}$  of CD3 stained with one drop of compensation beads, 1  $\mu\text{L}$  of CD26 stained with one drop of compensation beads, unstained cells, live and dead cells stained with 100  $\mu\text{L}$  of 1:3000 diluted eFluor 780. On day 6, 2  $\mu\text{L}$  of CD3 and CD56 and 3  $\mu\text{L}$  of  $\gamma\delta$  TCR per sample were required.

To undergo the staining protocol, 2 mL of PBS was added to each flow tube sample containing cells and spun down at 300 g for 5 minutes. Once the supernatants were discarded, the dead tube was placed on a 100°C heat block for 1 minute, then cooled at 4°C (on ice) for 1 minute before being combined with the dead tube. There was 100  $\mu\text{L}$  of eFluor added to each sample before being shaken for 20-30 minutes. Then 2 mL of PBS was added to each sample and the samples were centrifuged at 300 g for 5 minutes before the supernatants were aspirated. From here, 100  $\mu\text{L}$  of PBS, 1  $\mu\text{L}$  of CD3 antibody, 2  $\mu\text{L}$  of  $\gamma\delta$  TCR antibody, and 1  $\mu\text{L}$  of CD56 antibody were added to each tube. The samples were shaken at room temperature for 15 minutes. Then 2 mL of PBS was added and the samples were centrifuged at 300 x g for 5 minutes before the supernatant

was decanted. Another 100  $\mu$ L of PBS was added and then either the cells were immediately analyzed by flow cytometer or stored at 4°C until analysis was completed. In addition, on day 6, 1.5  $\mu$ L of 7-Aminoactinomycin D (7-AAD) was added a few minutes before data was analyzed by flow cytometry.

### **Freezing of $\gamma\delta$ T Cells**

The  $\gamma\delta$  T cells were counted and centrifuged at 250 g and room temperature for 10 minutes. Cells were resuspended in freezing media (5% HSA, 10% DMSO, and PBS) at a concentration of  $10^8$  cells/mL and aliquoted 1 mL per cryovial. The cells were transferred into a Mr. Frosty freezing container and stored at -80°C for 4 hours before being transferred to liquid nitrogen.

### **Thawing of $\gamma\delta$ T Cells**

The  $\gamma\delta$  T cells were thawed in a 37°C water bath until nearly completely thawed. Then 500  $\mu$ L of pre-warmed 5% HSA in 4 mL of PlasmaA was added in a dropwise fashion to cells. Cells were added to 8.5 mL of 5% HSA before being centrifuged at 250 g at room temperature for 10 minutes. After centrifugation, cells were resuspended in complete OpTmizer (40 mL OpTmizer + 404  $\mu$ L L-glut + 404  $\mu$ L Pen-Strep + 1.106 mL OpTmizer supplement) and 100 IU/mL IL-2 at a concentration of  $4 \times 10^6$  cells/mL. Cells were incubated for 2 hours at 37°C and 5% CO<sub>2</sub>.

### **Electroporation**

For each well of a 12-well plate, 1 mL of complete OpTmizer and IL-2 were added, then placed in the incubator. After counting, the cells were aliquoted into 1.5 mL Eppendorf tubes and PBS was added up to 1 mL. The cells were centrifuged at 250 g and room temperature for 10 minutes.



After the supernatant was discarded, the cells were resuspended in 1 mL of PBS. The cells were re-centrifuged at 250 g at room temperature for 10 minutes. After completely discarding the supernatant, including using a P100 or P20 tip to completely dry the pellet, the cells were resuspended in 100  $\mu$ L of Opti-MEM. Then 15  $\mu$ g of resuspended mRNA (encoding the plasmid for our CAR construct) was added. As a control, 10  $\mu$ L of water was added to cells that were mock electroporated. Then the cells were gently resuspended with a P100 pipet and transferred into 2 mm or 4 mm cuvettes before being electroporated using an electric field of 1000 V/cm, 1250 V/cm a voltage of 200 V or 500 V, a time gap of 2 ms or 5 ms or a Fisher or Biorad branded cuvette. Then 500  $\mu$ L of media were added to the cuvette before the cells were re-transferred to the 12-well plate. The cells were incubated overnight and measured approximately 24 hours post-transfection.

### **CAR Staining**

After the cell counts were taken, 100,000 cells were taken for each tube sample containing either the full stain or secondary alone, 50,000 cells were taken for the mock  $\gamma\delta$  T cells for the unstained control and for the live and dead tubes, and 50,000 cells were taken for the SCF CAR  $\gamma\delta$  T cells for the full-minus-one (FMO) stains. Then the cells were washed with 2 mL of FACS buffer and centrifuged at 320 g for 3 minutes. After centrifugation, the dead tube was killed by placement on a 100°C heat block for one minute before being placed on ice for one minute, then being combined with the live tube. Then 100  $\mu$ L of FACS buffer was added to all the tubes, and then 0.2  $\mu$ L of CD117-Fc was only added to the full-stained tubes. After vortexing, the cells were incubated at 4°C for 30 minutes. After, the cells were incubated, 2 mL of FACS buffer was added to each sample and the samples were centrifuged at 320 g for 3 minutes before the

supernatant was decanted. Then 100  $\mu$ L of FACS buffer was added to all the tubes, and 2 mL of secondary-PE was added to all the stained tubes before being vortexed. Then the cells were incubated in the cold room for 15 minutes. Once this was done, 2 mL of FACS buffer was added to each sample before the cells were centrifuged at 320 g for 3 minutes and the supernatant was discarded. Then 100  $\mu$ L of FACS buffer was added to all stained tubes, and for each stained tubes, 5  $\mu$ L of 1:1000 diluted eFluor780, 3  $\mu$ L of  $\gamma\delta$  TCR, 2  $\mu$ L of CD3, 2  $\mu$ L of CD56, and 2  $\mu$ L of CD16 were added. Then, each compensation tube contained 100  $\mu$ L of FACS buffer, 1 drop of beads, and either 1  $\mu$ L of  $\gamma\delta$  TCR, 1  $\mu$ L of CD56, 1  $\mu$ L of CD16, 1  $\mu$ L of CD3, or 1  $\mu$ L of CD3, unless it is an FMO tube in which all of them were contained except one. Then the samples were vortexed and incubated at 4°C for 20 minutes. Then 2 mL of FACS buffer was added to each sample and the samples were centrifuged at 320 g for 5 minutes before the supernatant was decanted. Finally, flow cytometry was run and at least 10,000 live events were collected.

## Results

### *Murine $\gamma\delta$ T Cell Expansion*

These experiments were performed in order to determine a protocol that would allow for the expansion of murine  $\gamma\delta$  T cells. This was done by retrieving male and female spleens, femurs, and tibias and performing cell culture. In order to determine expansion capability, metrics used included the number of  $\gamma\delta$  T cells, the percentage of  $\gamma\delta$  T cells in the culture, and the percentage of live cells in the culture. Patterns seen when devising these protocols included notable differences between murine  $\gamma\delta$  T cells from the spleen and the bone marrow and when using ConA as opposed to using CD3/CD28 beads, zoledronate, or LPS. In order to be considered an expansion, the murine  $\gamma\delta$  T cells should have an 80-fold expansion and a culture of 80% murine  $\gamma\delta$  T cells, as seen in the human  $\gamma\delta$  T cell expansion (Figure 20). The murine  $\gamma\delta$  T cells did not meet these criteria after our protocols.

### **Day 0 Murine $\gamma\delta$ T Cell Characteristics**

There are no significant differences in the number of  $\gamma\delta$  T cells harvested on day 0 between Balb/C mice and CD 45.1 Bl/6 mice. However, when comparing male bone marrow with male spleen or female bone marrow with female spleen in the Balb/C mice, you can see that within the same gender, the spleens contain greater numbers of  $\gamma\delta$  T cells than the bone marrow. No single organ can provide more than 1 million murine  $\gamma\delta$  T cells (Figure 4). There is a significant decrease in the percentage of  $\gamma\delta$  T cells within the same genders of bone marrow in Balb/C mice compared to CD45.1 Bl/6 mice. Within a CD 45.1 Bl/6 mouse, there are no significant differences between the percentage of murine  $\gamma\delta$  T cells between any organ. However, in a

Balb/C mouse, there is a significant increase in the percentage of murine  $\gamma\delta$  T cells in the female spleen compared to the female bone marrow. In contrast, in a Balb/C mouse, there are no significant differences in the percentage of murine  $\gamma\delta$  T cells in the male spleen compared to the male bone marrow (Figure 5).

### **Bead Activation**

CD3/CD28 beads were used for activation in experiments 1, 2, and 4 either on day 0 or day 3. On day 0, the percentage of murine  $\gamma\delta$  T cells ranged from 0.39-1.06% before the  $\alpha\beta$  depletion and 0.49-8.53% post-depletion (Figure 8). If they were able to survive past day 3 (data not shown), on experiment 1 day 7, the fold-expansion reached a maximum of 2.91 with male bone marrow or a minimum of 0.69 with the female spleen (Figure 7A). In fact, on Day 5, the fold expansion for male bone marrow reached 8.06 (Figure 7A, Figure 9). However, the percentage of  $\gamma\delta$  T cells on Day 7 ranged from 3.07–4.07%, where the percentage of  $\alpha\beta$  T cells was anywhere from 94.24–95.75% (Figure 10). Since the day 7 product was not majority  $\gamma\delta$  T cells, this activator was not able to isolate the  $\gamma\delta$  T cells.

### **Zoledronate Activation**

Zoledronate was used for activation in experiments 2 and 3. None of the cells were able to survive past day 3 (data not shown). Due to the low viability of the cells, we conclude that under our conditions, zoledronate did not expand murine  $\gamma\delta$  T cells from the spleen or bone marrow.

## LPS Activation

LPS was used for activation in experiments 4 and 5 either on day 0 or day 3. On day 0, the percentage of  $\gamma\delta$  T cells ranged from 0.67-0.95% (Figure 12). On day 7, the percentage of  $\gamma\delta$  T cells reached a highest of 4.38% with 2x LPS used for male bone marrow (Figure 11D). On experiment day 7, the highest fold-expansion after day 0 was on day 5 with 2x LPS female bone marrow and with 0.6330 fold-expansion (Figure 11D, Figure 13). Since the expansion did not reach above 2x expansion and the percentage of  $\gamma\delta$  T cells after the expansion is below 70%, means that LPS was not able to activate the murine  $\gamma\delta$  T cells.

In experiment 4, there was also a condition where LPS was used for activation on day 0 and CD3/CD28 was used for activation on day 3. By day 7, the male bone marrow didn't have enough cells to garner a sample. As for the percentage of  $\gamma\delta$  T cells, the male spleen condition had the highest percentage of  $\gamma\delta$  T cells at 34.4%, while the female bone marrow had the lowest percentage of  $\gamma\delta$  T cells at 8.54% (data not shown).

## ConA Activation

ConA was used for activation in experiments 6-9 on day 0 and once on day 3. Of the ConA experiments, on day 7, the highest percentage of  $\gamma\delta$  T cells we achieved was in experiment 7, where we achieved 69.0% of the cell culture being murine  $\gamma\delta$  T cells from a female spleen that was only activated once with ConA (data not shown). Similar results occurred on day 7 in the female spleen in experiment 6 (67.1%) (Figure 15C) but not in experiment 8 (34.5%) (Figure 16, Figure 17H) or experiment 9 (45.0%) (Figure 18, Figure 19H). As for the male spleens on day 7, experiment 6 yielded a percentage of 52.1% murine  $\gamma\delta$  T cells (Figure 15A) and experiment 9

yielded a percentage of 56.4% (Figure 19D), but experiment 8 yielded a percentage of 33.8% murine  $\gamma\delta$  T cells (Figure 17D). Since these values are highly variable and do not indicate any clear pattern, we cannot conclude that male spleens or female spleens provide a greater percentage of murine  $\gamma\delta$  T cells at the end of the proposed expansion.

Based on the results from experiment 6 day 7 with 1x ConA, seeing as there are 0% murine  $\gamma\delta$  T cells in male or female bone marrow (Figures 14B and 15B) compared to 52.1% in the male spleen (Figure 15A) and 67.1% in the female spleen, we can conclude that spleens expand with ConA better than bone marrow.

Considering that these percentages of murine  $\gamma\delta$  T cells are higher than the percentages achieved with CD3/CD28 beads, zoledronate, or LPS, we can conclude that of the activators we selected, murine  $\gamma\delta$  T cells are the best for isolating murine  $\gamma\delta$  T cells. We cannot say that the murine  $\gamma\delta$  T cells expand with ConA seeing as they do not reach above 2-fold expansion (the highest expansion of the ConA experiments being 1.99 fold expansion with female spleens by day 7 in experiment 6) (Figure 14A) and they do not reach above a percentage of 70% murine  $\gamma\delta$  T cells within the cell culture. This is low compared to our lab's human  $\gamma\delta$  T cell expansions, which are able to reach percentages of  $\gamma\delta$  T cells around 80% (Figure 20A) and 80-fold expansion (Sutton et al. 2016).

## *Human $\gamma\delta$ T cell Electroporation Protocol*

In addition to testing the expansion of murine  $\gamma\delta$  T cells, we also worked to optimize the electroporation of human  $\gamma\delta$  T cells to produce an SCF-CAR. These experiments were performed in order to determine a protocol that would allow for the transfection of human  $\gamma\delta$  T cells with mRNA encoding an SCF-CAR. This was done by expanding and freezing  $\gamma\delta$  T cells from acquired from blood donations (Figure 21), then thawing and transfecting the human  $\gamma\delta$  T cells (Figure 22). The variables that were used to determine the efficacy of this protocol included the balancing of CAR expression (as seen through %CAR+ cells and mean fluorescent intensity (MFI)) and viability (Table 2). Patterns seen when devising this protocol included seeing higher viabilities of SCF-CARs in Biorad cuvettes (Figure 23A) and the highest %CAR+ cells and MFI in Biorad 4 mm cuvettes that were electroporated for 2 milliseconds at 500 volts (Figure 23B and Figure 23C).

## Discussion

The first aim of our study was to determine a protocol to expand murine  $\gamma\delta$  T cells based on a published protocol by Williams (Williams et al. 2022). Seeing as we have developed a protocol for expanding human  $\gamma\delta$  T cells, we used those results to develop our criteria for murine  $\gamma\delta$  T cell expansion. If our criteria were met, the fold-expansion on day 7 would have reached 80 compared to day 0 and the percentage of  $\gamma\delta$  T cells in the cell culture would have reached 80%. This question was tested by using different activators and retrieving cells from different murine organs (Table 1). The goal of this study was to determine if murine  $\gamma\delta$  T cells from the bone marrow will migrate to the bone marrow and if murine  $\gamma\delta$  T cells from the spleen will migrate to the spleen.

When looking at our starting materials, the most prominent finding was that in Balb/C mice, male spleens had significantly more  $\gamma\delta$  T cells per organ than male bone marrow, and female spleens had significantly more  $\gamma\delta$  T cells per organ than female bone marrow. This means that when choosing between organs of Balb/C mice, it is best to harvest the spleens rather than the bone marrow. Future studies could focus on why this is the case, and if murine bone marrow cells respond to different activators than murine spleen cells. There was no clear pattern seen in the percentage or number of murine  $\gamma\delta$  T cells when separating by age (as measured from 4-8 weeks old) (Figure 6).

We initially experimented with using CD3/CD28 beads to expand murine  $\gamma\delta$  T cells on either day 0 or day 3, similar to the published protocol by Williams (Williams et al. 2022). This protocol provided some of the highest rates of fold expansion we saw throughout these experiments.



However, seeing as our product from experiment 1 was almost entirely composed of  $\alpha\beta$  T cells rather than  $\gamma\delta$  T cells, even after an  $\alpha\beta$  depletion on day 0, we concluded that this would not expand murine  $\gamma\delta$  T cells. This is likely due to the fact that CD3/CD28 will target all T cells, including both murine  $\alpha\beta$  T cells and  $\gamma\delta$  T cells. If there is originally a smaller percentage of  $\gamma\delta$  T cells than  $\alpha\beta$  T cells and the activator is not specific for  $\gamma\delta$  T cells, even after the activation, the  $\gamma\delta$  T cells will continue to share a smaller proportion of the product if the activator. These beads will cause expansion of all T cells, including  $\alpha\beta$  T cells.

Next, we decided to test zoledronate, as it has been successfully used in our lab to expand human  $\gamma\delta$  T cells. However, whenever our experiments used zoledronate on day 0, they died by 3 three, whether or not an  $\alpha\beta$  depletion occurred on day 0 or day 3. While zoledronate may expand human  $\gamma\delta$  T cells, zoledronate does not expand murine  $\gamma\delta$  T cells. This is likely because human  $\gamma\delta$  T cells are part of the V $\delta$ 2 subset while the murine  $\gamma\delta$  T cells are of the V $\gamma$ 1 subtype. Likely, the V $\gamma$ 1 subtype does not respond to bisphosphonates.

Our next activator was LPS. Due to low percentages of  $\gamma\delta$  T cells and fold expansion, we concluded that LPS is unable to expand murine  $\gamma\delta$  T cells. While we did see some results, perhaps LPS simply isn't strong enough on its own to manage a robust response for  $\gamma\delta$  T cells and needs to be combined with other activators.

Finally, we used ConA to activate murine  $\gamma\delta$  T cells. This activator had the highest percentages of murine  $\gamma\delta$  T cells that were present in the cell culture. However, the fold expansion and the number of murine  $\gamma\delta$  T cells in the culture were not optimal for further experimentation, where

we would preferably need 10 million  $\gamma\delta$  T cells. In this way, ConA is best at isolating  $\gamma\delta$  T cells compared to the other activators, but it is still unable to expand murine  $\gamma\delta$  T cells. Another condition that improves the ability of ConA to produce murine  $\gamma\delta$  T cells includes harvesting murine  $\gamma\delta$  T cells from spleens rather than bone marrow. While ConA is able to increase the percentage of murine  $\gamma\delta$  T cells in culture, perhaps another activator is needed in order to increase the fold-expansion of the murine  $\gamma\delta$  T cells.

To further this investigation of  $\gamma\delta$  T cells, we wanted to test our lab's previously developed, FDA-compliant method for expanding human  $\gamma\delta$  T cells. To enhance their killing ability, we developed a protocol to optimize the genetic engineering of these cells using transfection technologies. After collecting blood samples from human donors and isolating the PBMCs, we performed an  $\alpha\beta$  T cell depletion on day 6 before freezing them down for cryopreservation on day 14. When required for experiments, they were thawed and electroporated. The next day, flow cytometry analysis was done to determine the success of the electroporation using metrics such as viability, %CAR+ Expression, and MFI. Since its high viability and CAR expression were relatively higher compared to the other experimental conditions, the Biorad 4 mm cuvettes electroporated for 2 ms at 500 volts were considered to be the optimal condition.

Future studies could expand on our work on attempting to expand murine  $\gamma\delta$  T cells by conditioning the mouse before harvesting organs. Previous studies have shown that humans who exercise are more likely to have their  $\gamma\delta$  T cell populations expand (Burnham et al. 2020). This could be implemented with mice through enrichment activities such as monitored time with an exercise wheel and recording how long they use it. Another route we could also consider is

injecting the mouse *in vivo* with our activating agent a few days before harvesting the organs to increase the number and/or percentage of murine  $\gamma\delta$  T cells harvested before *in vitro* culturing techniques.

Considering the novel implications of CAR T cell therapy for curing deadly diseases and the new forms of CARs currently in development, it is imperative we have a syngeneic mouse model ready for testing. This experiment has shown examples of activators that will increase the percentage of *in vitro* murine  $\gamma\delta$  T cells from the spleen and bone marrow. While more work must be done to produce a true expansion, we now have a framework of different parameters that can be tested to optimize an expansion such as this. Furthermore, the optimization of the transfection protocol for human  $\gamma\delta$  T cells will allow for an off-the-shelf, bulk production of SCF-CAR T cells, ultimately cutting costs and treatment wait times for patients.

## References

- Benjamin, Reuben, Charlotte Graham, Deborah Yallop, Agnieszka Jozwik, Oana C Mirci-Danicar, Giovanna Lucchini, Danielle Pinner, et al. 2020. "Genome-Edited, Donor-Derived Allogeneic Anti-CD19 Chimeric Antigen Receptor T Cells in Paediatric and Adult B-Cell Acute Lymphoblastic Leukaemia: Results of Two Phase 1 Studies." *The Lancet* 396 (10266): 1885–94. [https://doi.org/10.1016/S0140-6736\(20\)32334-5](https://doi.org/10.1016/S0140-6736(20)32334-5).
- Benjamin, Reuben, Nitin Jain, Marcela V. Maus, Nicolas Boissel, Charlotte Graham, Agnieszka Jozwik, Deborah Yallop, et al. 2022. "UCART19, a First-in-Class Allogeneic Anti-CD19 Chimeric Antigen Receptor T-Cell Therapy for Adults with Relapsed or Refractory B-Cell Acute Lymphoblastic Leukaemia (CALM): A Phase 1, Dose-Escalation Trial." *The Lancet Haematology* 9 (11): e833–43. [https://doi.org/10.1016/S2352-3026\(22\)00245-9](https://doi.org/10.1016/S2352-3026(22)00245-9).
- Branella, Gianna M., and Harold Trent Spencer. 2021. "Natural Receptor- and Ligand-Based Chimeric Antigen Receptors: Strategies Using Natural Ligands and Receptors for Targeted Cell Killing." *Cells* 11 (1): 21. <https://doi.org/10.3390/cells11010021>.
- Burnham, Rebecca E., Jaquelyn T. Zoine, Jamie Y. Story, Swetha N. Garimalla, Greg Gibson, Aaron Rae, Erich Williams, et al. 2020. "Characterization of Donor Variability for  $\Gamma\delta$  T Cell Ex Vivo Expansion and Development of an Allogeneic  $\Gamma\delta$  T Cell Immunotherapy." *Frontiers in Medicine* 7 (November): 588453. <https://doi.org/10.3389/fmed.2020.588453>.
- Chiarella, Emanuela, Bruna Codispoti, Annamaria Aloisio, Emanuela G. Cosentino, Stefania Scicchitano, Ylenia Montalcini, Daniela Lico, Giovanni Morrone, Maria Mesuraca, and Heather M. Bond. 2020. "Zoledronic Acid Inhibits the Growth of Leukemic MLL-AF9 Transformed Hematopoietic Cells." *Heliyon* 6 (6): e04020. <https://doi.org/10.1016/j.heliyon.2020.e04020>.
- Döhner, Hartmut, Daniel J. Weisdorf, and Clara D. Bloomfield. 2015. "Acute Myeloid Leukemia." *New England Journal of Medicine* 373 (12): 1136–52. <https://doi.org/10.1056/NEJMra1406184>.
- Gill, Saar, Marcela V. Maus, and David L. Porter. 2016. "Chimeric Antigen Receptor T Cell Therapy: 25years in the Making." *Blood Reviews* 30 (3): 157–67. <https://doi.org/10.1016/j.blre.2015.10.003>.
- Gross, G, T Waks, and Z Eshhar. 1989. "Expression of Immunoglobulin-T-Cell Receptor Chimeric Molecules as Functional Receptors with Antibody-Type Specificity." *Proceedings of the National Academy of Sciences of the United States of America* 86 (24): 10024–28. <https://www.ncbi.nlm.nih.gov/pmc/articles/PMC298636/>.
- Jagannathan-Bogdan, Madhumita, and Leonard I. Zon. 2013. "Hematopoiesis." *Development (Cambridge, England)* 140 (12): 2463–67. <https://doi.org/10.1242/dev.083147>.

- Jhita, Navdeep, and Sunil S. Raikar. 2022. "Allogeneic Gamma Delta T Cells as Adoptive Cellular Therapy for Hematologic Malignancies." *Exploration of Immunology* 2 (3): 334–50. <https://doi.org/10.37349/ei.2022.00054>.
- Kochenderfer, James N., Robert P. T. Somerville, Tangying Lu, James C. Yang, Richard M. Sherry, Steven A. Feldman, Lori McIntyre, et al. 2017. "Long-Duration Complete Remissions of Diffuse Large B Cell Lymphoma after Anti-CD19 Chimeric Antigen Receptor T Cell Therapy." *Molecular Therapy* 25 (10): 2245–53. <https://doi.org/10.1016/j.ymthe.2017.07.004>.
- Leick, Mark B., Harrison Silva, Irene Scarfò, Rebecca Larson, Bryan D. Choi, Amanda A. Bouffard, Kathleen Gallagher, et al. 2022. "Non-Cleavable Hinge Enhances Avidity and Expansion of CAR-T Cells for Acute Myeloid Leukemia." *Cancer Cell* 40 (5): 494-508.e5. <https://doi.org/10.1016/j.ccell.2022.04.001>.
- Malaise, Muriel, Daniel Steinbach, and Selim Corbacioglu. 2009. "Clinical Implications of C-Kit Mutations in Acute Myelogenous Leukemia." *Current Hematologic Malignancy Reports* 4 (2): 77–82. <https://doi.org/10.1007/s11899-009-0011-8>.
- Mardiana, Sherly, and Saar Gill. 2020. "CAR T Cells for Acute Myeloid Leukemia: State of the Art and Future Directions." *Frontiers in Oncology* 10 (May): 697. <https://doi.org/10.3389/fonc.2020.00697>.
- Morath, Anna, and Wolfgang W. Schamel. 2020. "A $\beta$  and  $\Gamma\delta$  T Cell Receptors: Similar but Different." *Journal of Leukocyte Biology* 107 (6): 1045–55. <https://doi.org/10.1002/JLB.2MR1219-233R>.
- Petersdorf, Effie W. 2013. "The Major Histocompatibility Complex: A Model for Understanding Graft-versus-Host Disease." *Blood* 122 (11): 1863–72. <https://doi.org/10.1182/blood-2013-05-355982>.
- Poltorak, A., X. He, I. Smirnova, M. Y. Liu, C. Van Huffel, X. Du, D. Birdwell, et al. 1998. "Defective LPS Signaling in C3H/HeJ and C57BL/10ScCr Mice: Mutations in Tlr4 Gene." *Science (New York, N.Y.)* 282 (5396): 2085–88. <https://doi.org/10.1126/science.282.5396.2085>.
- Qu, Guanyu, Shengli Wang, Zhenlong Zhou, Dawei Jiang, Aihua Liao, and Jing Luo. 2022. "Comparing Mouse and Human Tissue-Resident  $\Gamma\delta$  T Cells." *Frontiers in Immunology* 13. <https://www.frontiersin.org/articles/10.3389/fimmu.2022.891687>.
- Rafiq, Sarwish, Oladapo O. Yeku, Hollie J. Jackson, Terence J. Purdon, Dayenne G. van Leeuwen, Dylan J. Drakes, Mei Song, et al. 2018. "Targeted Delivery of a PD-1-Blocking ScFv by CAR-T Cells Enhances Anti-Tumor Efficacy in Vivo." *Nature Biotechnology* 36 (9): 847–56. <https://doi.org/10.1038/nbt.4195>.

- Razavi, Azadeh Sadat, Angelica Loskog, Sepideh Razi, and Nima Rezaei. 2023. "The Signaling and the Metabolic Differences of Various CAR T Cell Designs." *International Immunopharmacology* 114 (January): 109593. <https://doi.org/10.1016/j.intimp.2022.109593>.
- Richards, Jackson R., Jae Hyuk Yoo, Donghan Shin, and Shannon J. Odelberg. 2020. "Mouse Models of Uveal Melanoma: Strengths, Weaknesses, and Future Directions." *Pigment Cell & Melanoma Research* 33 (2): 264–78. <https://doi.org/10.1111/pcmr.12853>.
- Rubnitz, Jeffrey E., Bassem I. Razzouk, Shelly Lensing, Stanley Pounds, Ching-Hon Pui, and Raul C. Ribeiro. 2007. "Prognostic Factors and Outcome of Recurrence in Childhood Acute Myeloid Leukemia." *Cancer* 109 (1): 157–63. <https://doi.org/10.1002/cncr.22385>.
- Salter, Alexander I., Margot J. Pont, and Stanley R. Riddell. 2018. "Chimeric Antigen Receptor–Modified T Cells: CD19 and the Road Beyond." *Blood* 131 (24): 2621–29. <https://doi.org/10.1182/blood-2018-01-785840>.
- Saura-Esteller, José, Milon de Jong, Lisa A. King, Erik Ensing, Benjamin Winograd, Tanja D. de Gruijl, Paul W. H. I. Parren, and Hans J. van der Vliet. 2022. "Gamma Delta T-Cell Based Cancer Immunotherapy: Past-Present-Future." *Frontiers in Immunology* 13. <https://www.frontiersin.org/articles/10.3389/fimmu.2022.915837>.
- Siegers, Gabrielle M., Helena Dhamko, Xing-Hua Wang, A. Mark Mathieson, Yoko Kosaka, Tania C. Felizardo, Jeffrey A. Medin, et al. 2011. "Human V $\delta$ 1  $\Gamma\delta$  T Cells Expanded from Peripheral Blood Exhibit Specific Cytotoxicity against B-Cell Chronic Lymphocytic Leukemia-Derived Cells." *Cytotherapy* 13 (6): 753–64. <https://doi.org/10.3109/14653249.2011.553595>.
- Sutton, Kathryn S., Anindya Dasgupta, David McCarty, Christopher B. Doering, and H. Trent Spencer. 2016. "Bioengineering and Serum Free Expansion of Blood-Derived  $\Gamma\delta$  T Cells." *Cytotherapy* 18 (7): 881–92. <https://doi.org/10.1016/j.jcyt.2016.04.001>.
- Tassone, P., P. Neri, R. Burger, M. T. Di Martino, E. Leone, N. Amodio, M. Caraglia, and P. Tagliaferri. 2012. "Mouse Models as a Translational Platform for the Development of New Therapeutic Agents in Multiple Myeloma." *Current Cancer Drug Targets* 12 (7): 814–22. <https://doi.org/10.2174/156800912802429292>.
- Torikai, Hiroki, and Laurence JN Cooper. 2016. "Translational Implications for Off-the-Shelf Immune Cells Expressing Chimeric Antigen Receptors." *Molecular Therapy* 24 (7): 1178–86. <https://doi.org/10.1038/mt.2016.106>.
- Ung, Emilie C, Gianna M Branella, and H Trent Spencer. 2022. "Optimizing Ligand-Based CAR Expression in  $\Gamma\delta$  T Cells," 1.
- Williams, Lindsay, Kenneth J. Dery, Wen-Hui Lee, Harry Li, John E. Shively, and Maciej Kujawski. 2022. "Isolation and Expansion of Murine  $\Gamma\delta$  T Cells from Mouse

Splenocytes.” *Journal of Immunological Methods* 508 (September): 113322.  
<https://doi.org/10.1016/j.jim.2022.113322>.

Zsebo, K. M., D. A. Williams, E. N. Geissler, V. C. Broudy, F. H. Martin, H. L. Atkins, R. Y. Hsu, N. C. Birkett, K. H. Okino, and D. C. Murdock. 1990. “Stem Cell Factor Is Encoded at the Sl Locus of the Mouse and Is the Ligand for the C-Kit Tyrosine Kinase Receptor.” *Cell* 63 (1): 213–24. [https://doi.org/10.1016/0092-8674\(90\)90302-u](https://doi.org/10.1016/0092-8674(90)90302-u).

## Figures

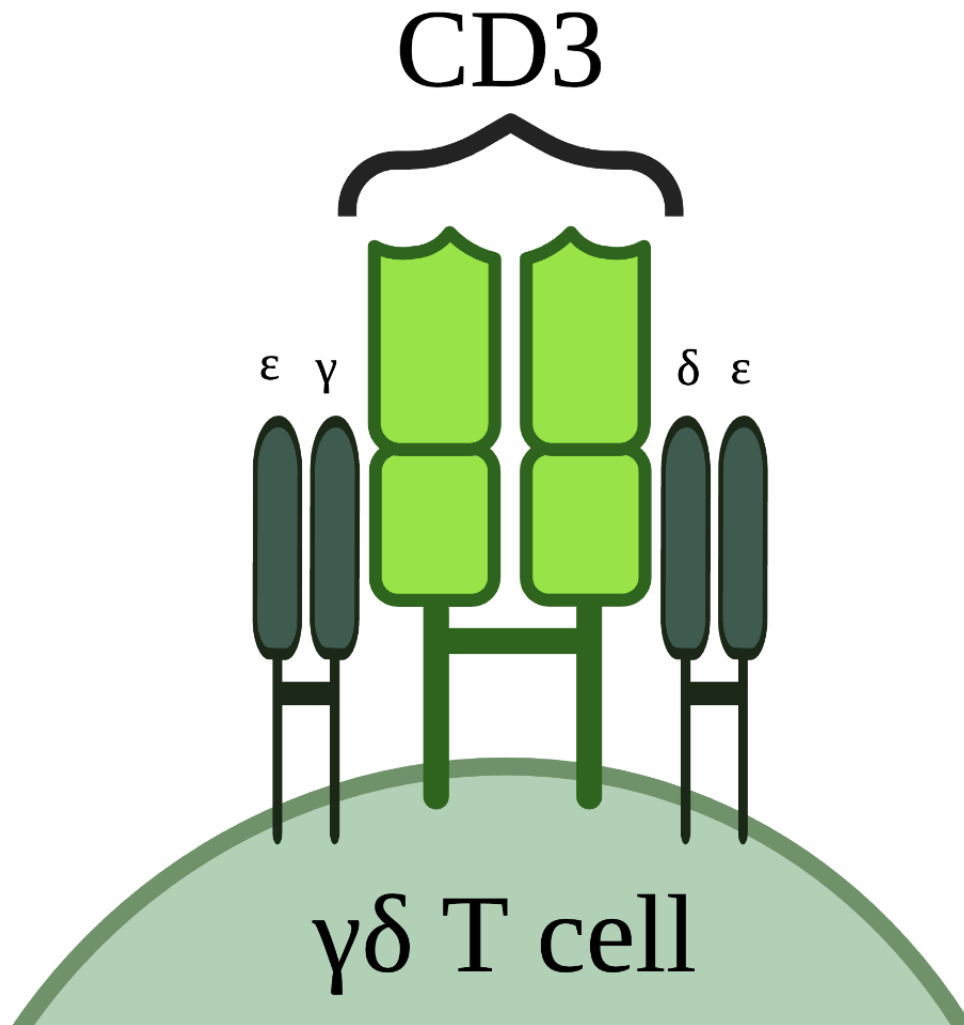


**Figure 1.** This is an example of a  $\gamma\delta$  T cell receptor. The CD3 receptor is what defines a T cell. The gamma and delta portions on either side of the CD3 receptor as well as the binding sequence of the TCR are what define this T cell to be of the  $\gamma\delta$  variety. Created with BioRender.com.



# Ligand-Based Chimeric Antigen Receptor (CAR)

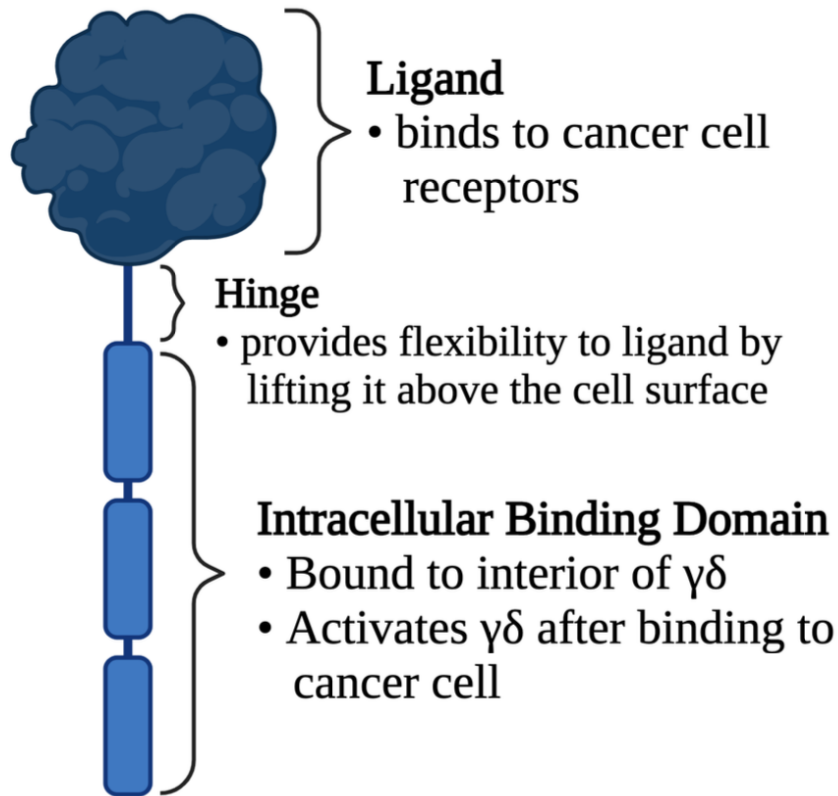


**Figure 2.** A diagram detailing the various portions of a ligand-based CAR. In this experiment, we used an SCF as our ligand. Taken from a presentation from our lab (Ung, Branella, and Spencer 2022). Created with BioRender.com.

# Murine $\gamma\delta$ T Cell Expansion Timeline ConA

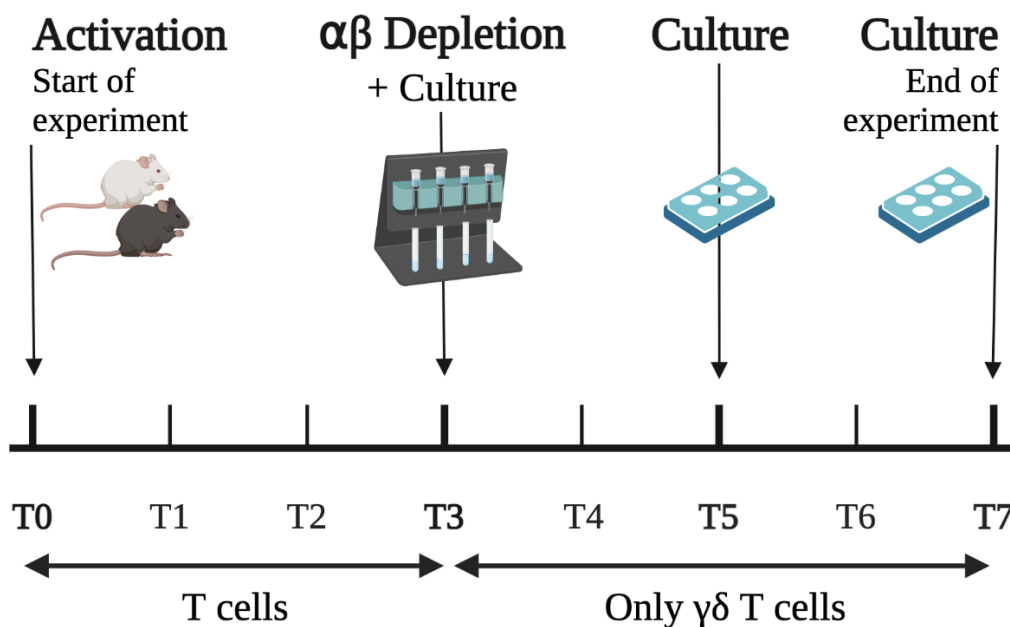


**Figure 3.** This diagram details the major steps this protocol required to attempt to expand murine  $\gamma\delta$  T cells using ConA. On Day 0, the spleen was harvested from either the Balb/C or the CD45.1 Bl/6 mice and the cells are activated with ConA. On Day 3, an  $\alpha\beta$  depletion occurred via a magnetic negative selection, which allowed us to culture  $\gamma\delta$  T cells for the rest of the protocol. On days 0, 3, 5, and 7, the  $\gamma\delta$  T cells were cultured and analyzed via flow. Created with BioRender.com.

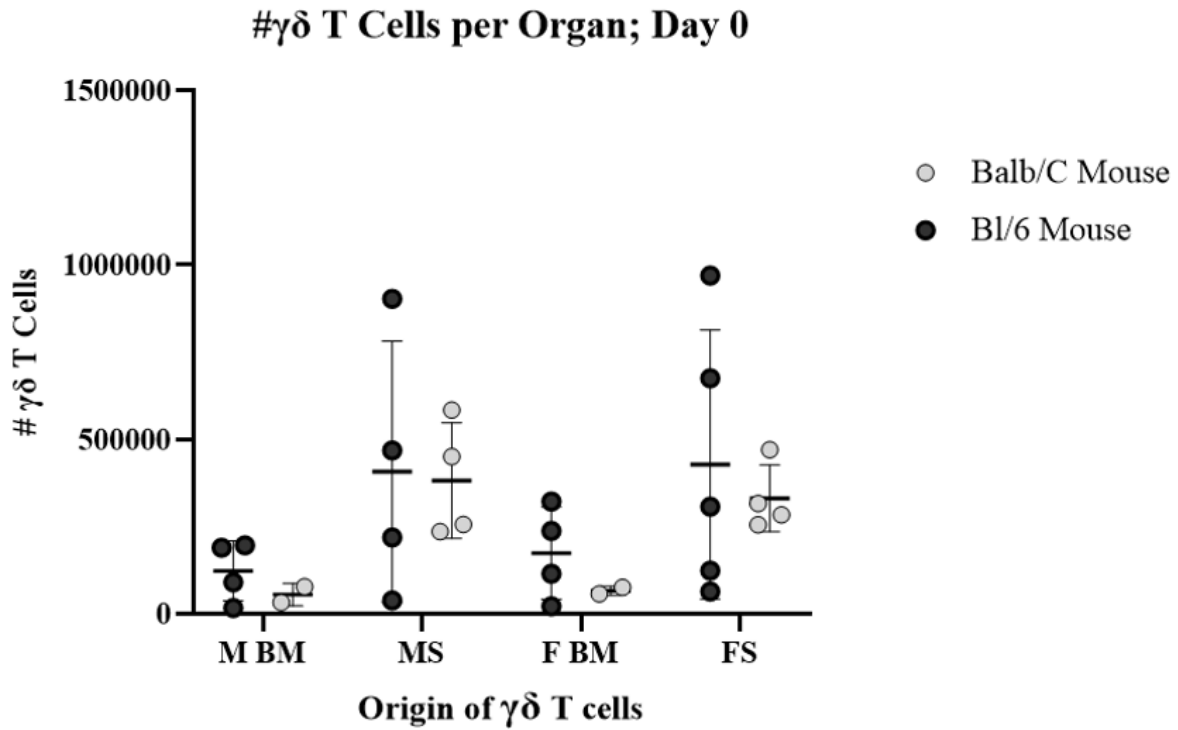


**Figure 4.** This graph shows the number of  $\gamma\delta$  T cells harvested from male and female bones and spleens on day 0 from each experiment, as stratified by mouse strain.

Key: M BM = male bone marrow; MS = male spleen; F BM = female bone marrow; FS = female spleen. These acronyms continue for the rest of the figures.

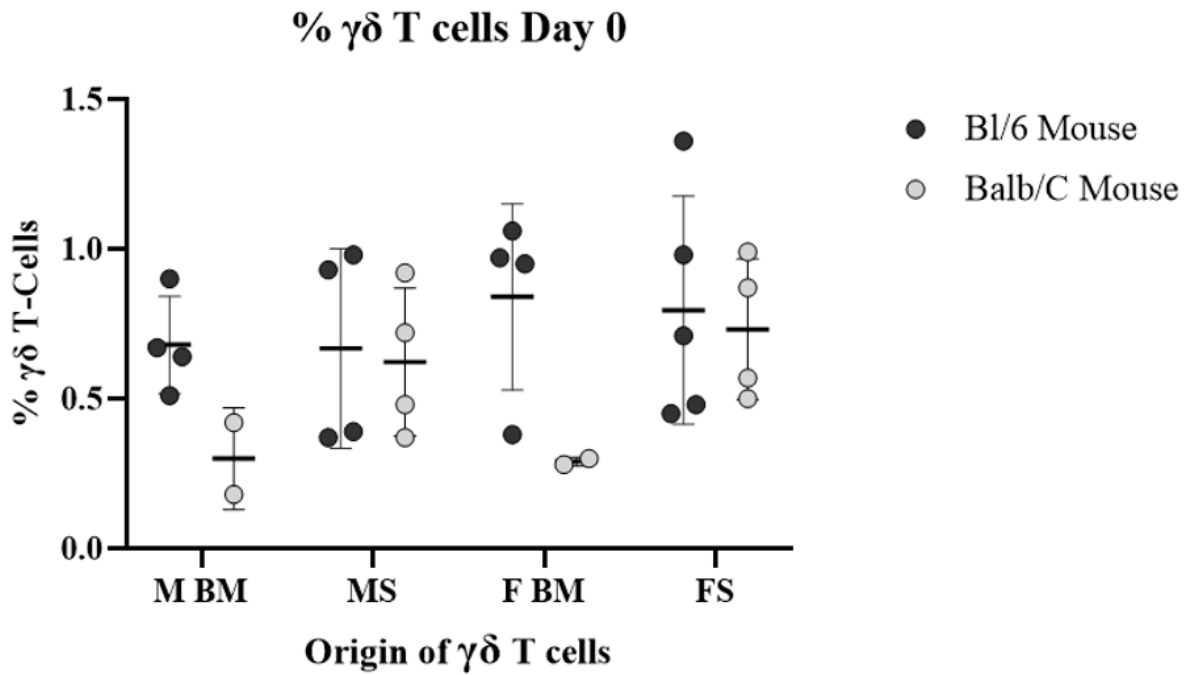


**Figure 5.** This graph shows the percentage of  $\gamma\delta$  T cells harvested from male and female bone marrow and spleens on day 0 from each experiment, as stratified by mouse strain.

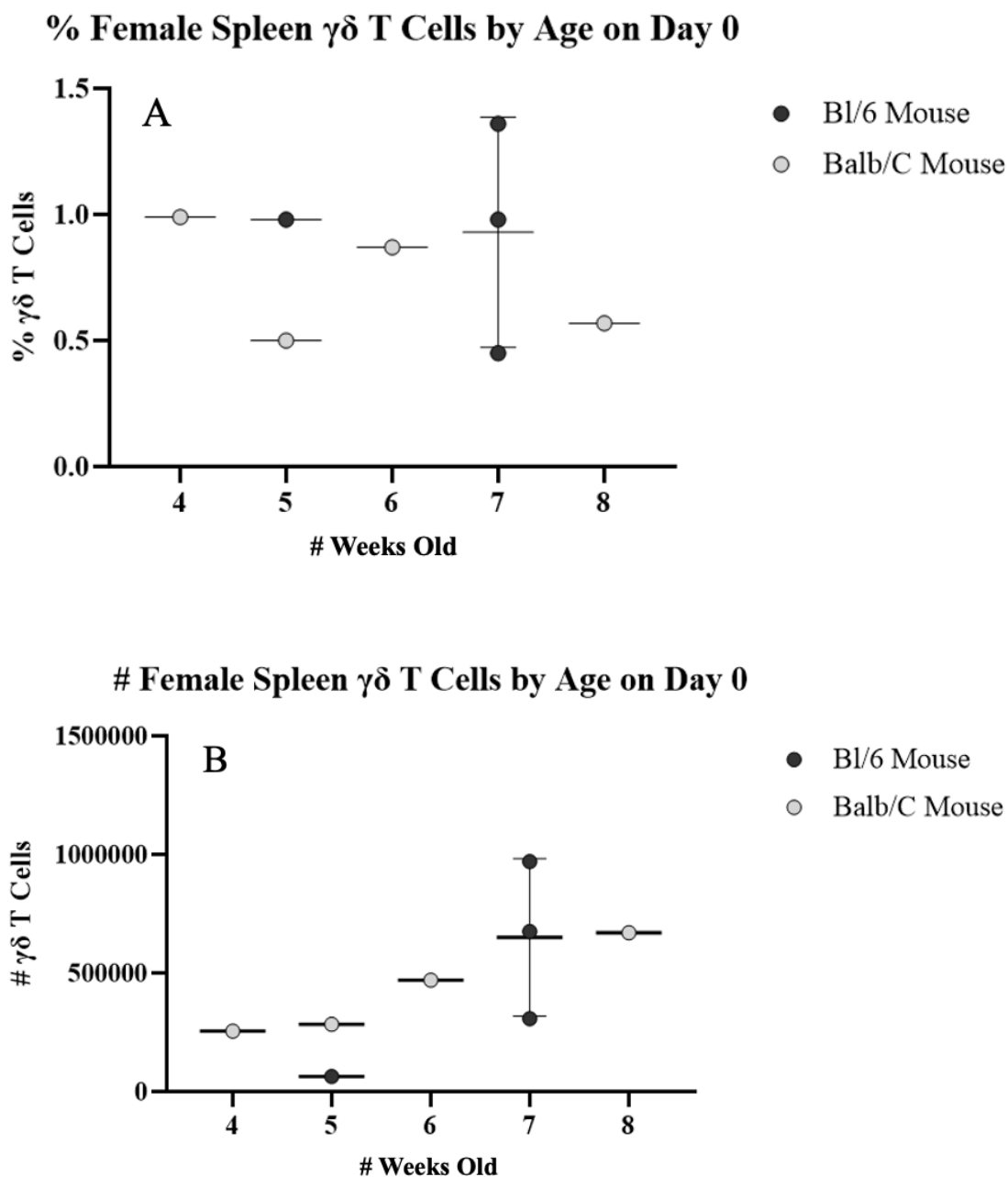


**Figure 6.** These graphs display the percentages (A) and numbers (B) of  $\gamma\delta$  T cells retrieved from female spleens, as divided by the ages of the mice. There do not appear to be any clear patterns relating the percentage or number of murine  $\gamma\delta$  T cells with age, whether or not you consider the mouse strains. The greatest percentage of  $\gamma\delta$  T cells was seen in a CD45.1 Bl/6 mouse at 1.36% while the greater number of  $\gamma\delta$  T cells was seen in a Bl/6 mouse at  $9.70 \times 10^5$   $\gamma\delta$  T cells. These two statistics did not come from the same individual mouse.

Experiment #	Mouse Strain	Age (weeks)	Media Contents	Gender + Organ for Experimental Groups	Activation Strategy	Antibodies and Beads used for Negative Selection	Depletion Column Used	Day of Depletion	Day 0 Cultured Concentration (cells/mL)	Day 3-7 Cultured Concentrations (cells/mL)	IL-2 on Day 0 (IU/mL)	IL-2 on Day 3-7 (IU/mL)
1	Bl/6 CD45.1	5	RPMI, 10% FBS, 1% Pen-Strep, 1% sodium-pyruvate, 1% MEM NEAA, 1% L-glutamine, 0.00002% of $\beta$ -ME	M BM, MS, F BM, FS, only obtained the femurs for BM	25 $\mu$ L of CD3/CD28 Beads per $10^6$ cells on Day 0	Biotin anti-CD11b, Biotin anti-B220, Biotin anti-CD4, & Biotin anti-CD8 antibodies at 0.1 $\mu$ L/mL and 20 $\mu$ L anti-Biotin beads per $10^7$ cells	LS	0	$2 \times 10^6$	$5 \times 10^5$	100	100
2	Bl/6 CD45.1	7	Same as experiment 1	M BM, MS, F BM, FS	6.25 $\mu$ L of CD3/CD28 Beads per $10^6$ cells or 1.67 $\mu$ L of Zol/mL of media on Day 0	Biotin anti-CD4 & Biotin anti-CD8 antibodies at 10 $\mu$ L/mL and 20 $\mu$ L anti-Biotin beads per $10^7$ cells	LD	0	$2 \times 10^6$	$5 \times 10^5$	100	100
3	Balb/C	6	Same as experiment 1	M BM, MS, F BM, FS	1.67 $\mu$ L of Zol/mL of media on Day 0	N/A	N/A	N/A	$1 \times 10^6$	N/A	500	N/A
4	Bl/6 CD45.1	7	Same as experiment 1	M BM, MS, F BM, FS	1 $\mu$ g LPS/mL of media on Day 0, 25 $\mu$ L of CD3/CD28 Beads per $10^6$ cells or no activation on Day 3	Biotin anti-CD4 & Biotin anti-CD8 antibodies at 10 $\mu$ L/mL and 20 $\mu$ L anti-Biotin beads per $10^7$ cells	LD	3	$4 \times 10^6$	$2 \times 10^6$	500	1000
5	Bl/6 CD45.1	no data	Same as experiment 1	M BM, MS, F BM, FS	1 $\mu$ g LPS/mL of media on Day 0 or on both Day 0 & Day 3	Biotin anti-CD4 & Biotin anti-CD8 antibodies at 10 $\mu$ L/mL and 20 $\mu$ L anti-Biotin beads per $10^7$ cells	LD	3	$1 \times 10^6$	$2 \times 10^6$	500	1000
6	Balb/C	5	RPMI, 10% FBS, 1% Pen-Strep, 3% ATOS	M BM, MS, F BM, FS	4 $\mu$ g ConA/mL of media on Day 0 or both Day 0 & Day 3	Biotin anti-TCR $\beta$ at 10 $\mu$ L/mL and 20 $\mu$ L anti-PE microbeads per $10^7$ cells	LD	3	$5 \times 10^6$	$3 \times 10^6$	500	1000
7	Bl/6 CD45.1	7	Same as Experiment 6	FS	4 $\mu$ g ConA/mL of media on Day 0	Biotin anti-CD4 & Biotin anti-CD8 antibodies at 10 $\mu$ L/mL and 20 $\mu$ L anti-Biotin beads per $10^7$ cells	LD	3	$5 \times 10^6$	$5 \times 10^6$	500	1000
8	Balb/C	8	Same as Experiment 6	MS, FS, MS + FS, MS in FS media	4 $\mu$ g ConA/mL of media on Day 0	Biotin anti-CD4 & Biotin anti-CD8 antibodies at 10 $\mu$ L/mL and 20 $\mu$ L anti-Biotin beads per $10^7$ cells	LD	3	$3.7 \times 10^6$	$5 \times 10^6$	500	1000
9	Balb/C	4	Same as Experiment 6	MS (noticeably larger than usual), FS	4 $\mu$ g ConA/mL of media on Day 0	Biotin anti-CD4 & Biotin anti-CD8 antibodies at 10 $\mu$ L/mL and 20 $\mu$ L anti-Biotin beads per $10^7$ cells	LD	3	$5 \times 10^6$	$3 \times 10^6$	500	1000

**Table 1.** This table describes the various parameters that were changed between each experiment. Experiment 1 was modified from a paper by Williams (Williams et al. 2022). Experiments 1-4 showed the most variability between experiments as they were intended to compare multiple variables at once, and the experiments were also adjusted to become more similar to our human  $\gamma\delta$  T cell expansion protocol. Experiments 6-9, showed the least variability in these parameters as some favorable results had started to emerge, and therefore the following experiments was focused on replicating those results.

Key: M BM = male bone marrow, MS = male spleen, F BM = female bone marrow, FS = female spleen, Zol = zoledronate, PE = phycoerythrin

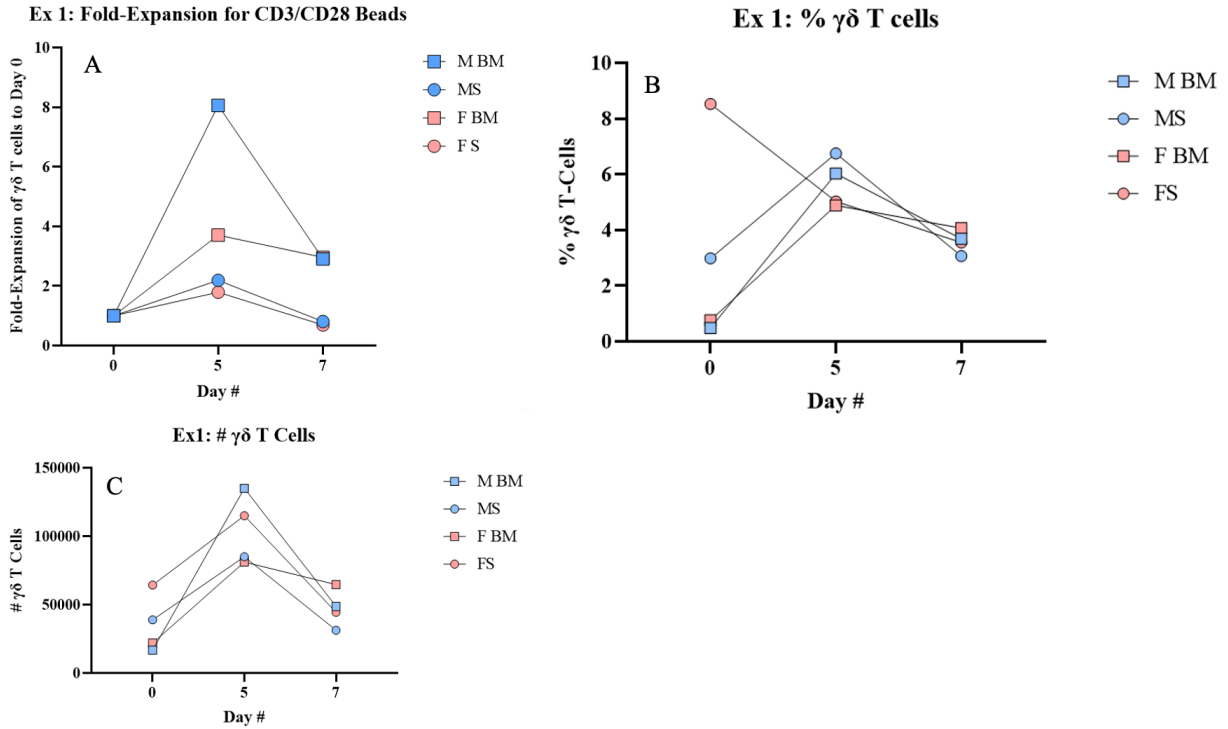


**Figure 7.** This graph shows the experimental results after the attempted expansion of murine  $\gamma\delta$  T cells using CD3/CD28 beads. The fold expansion (A), percentage (B), and number (B) of murine  $\gamma\delta$  T cells appear to peak on day 5 with the exception of the percentage of murine  $\gamma\delta$  T cells in the female spleen, which peaked on day 0.

Gating Strategy:

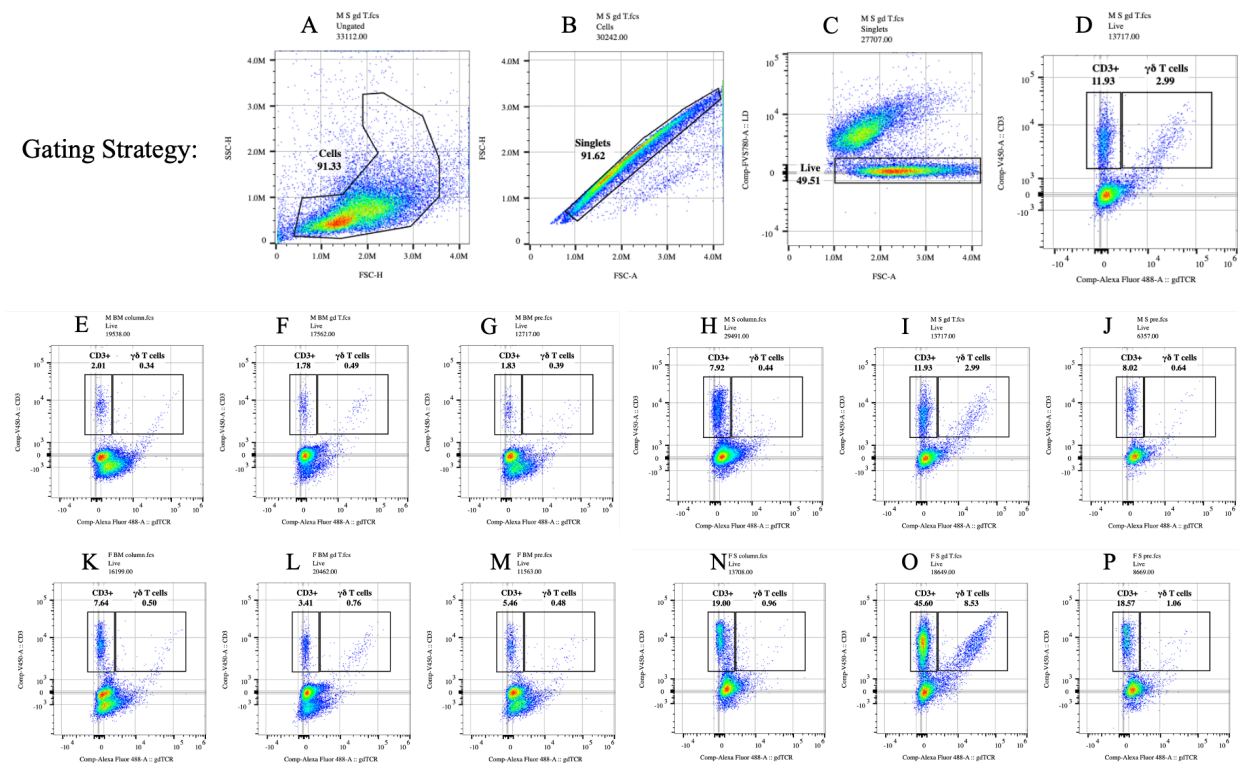


**Figure 8.** This graph displays the flow cytometry analysis on experiment 1 day 0 of the murine  $\gamma\delta$  T cell attempt at expansion with CD3/CD28 beads. Graphs A-D show the gating strategy for male spleen where cells were gated, then single cells, then the live cells, then the CD3+ cells (T cells), the  $\gamma\delta$  T cells, and each of their respective percentages. Graphs E-P show the flow plots of male bone marrow, male spleen, female bone marrow, and female spleen that came from the column used for the depletion (E, H, K, N), were purified due to going through the column (F, I, L, O), and before the column depletion (G, J, M, P).



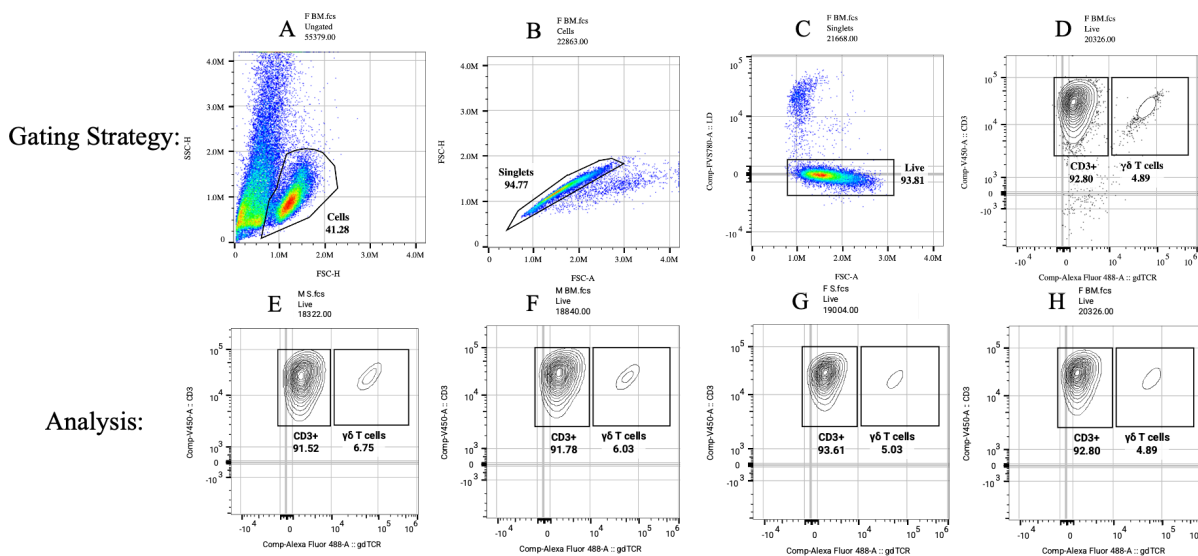


**Figure 9.** This graph shows the flow cytometry analysis for experiment 1 day 5 of the murine  $\gamma\delta$  T cell attempt at expansion using CD3/CD28 beads. Graphs A-D show the gating strategy for female bone marrow and graphs E-H show the percentages of CD3+ and  $\gamma\delta$  T cells. The percentage of CD3+ T cells hovers around 92% while the percentage of murine  $\gamma\delta$  T cells never reaches above 6.75%.

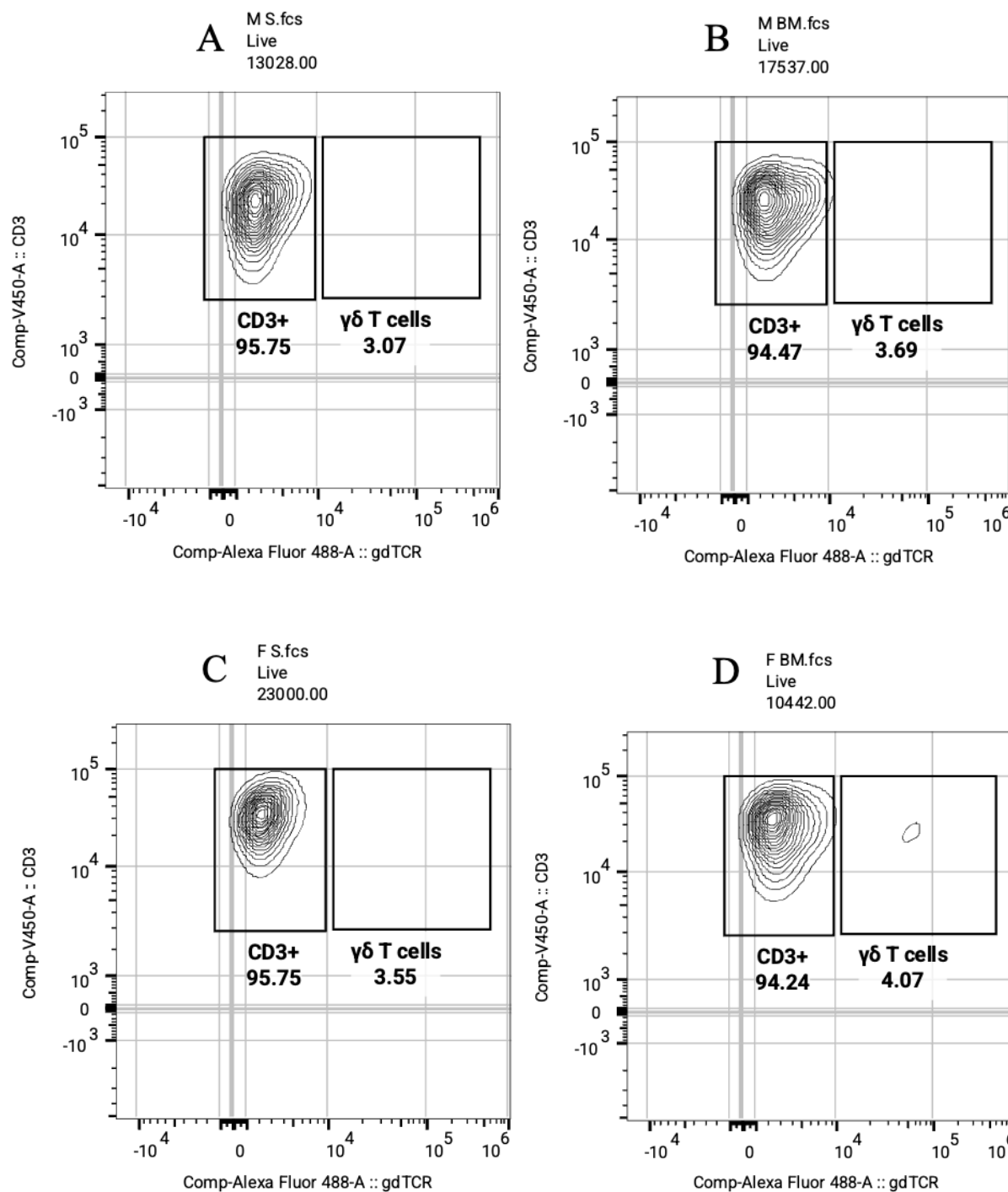


**Figure 10.** This graph shows the flow cytometry analysis on experiment 1 day 7 of the murine  $\gamma\delta$  T cells attempted expansion using CD3/CD28 beads. Figures A-D display the percentages of murine CD3+ and  $\gamma\delta$  T cells. The percentages of CD3+ cells hovers around 95% while the percentages of  $\gamma\delta$  T cells never strays above 4.07%.

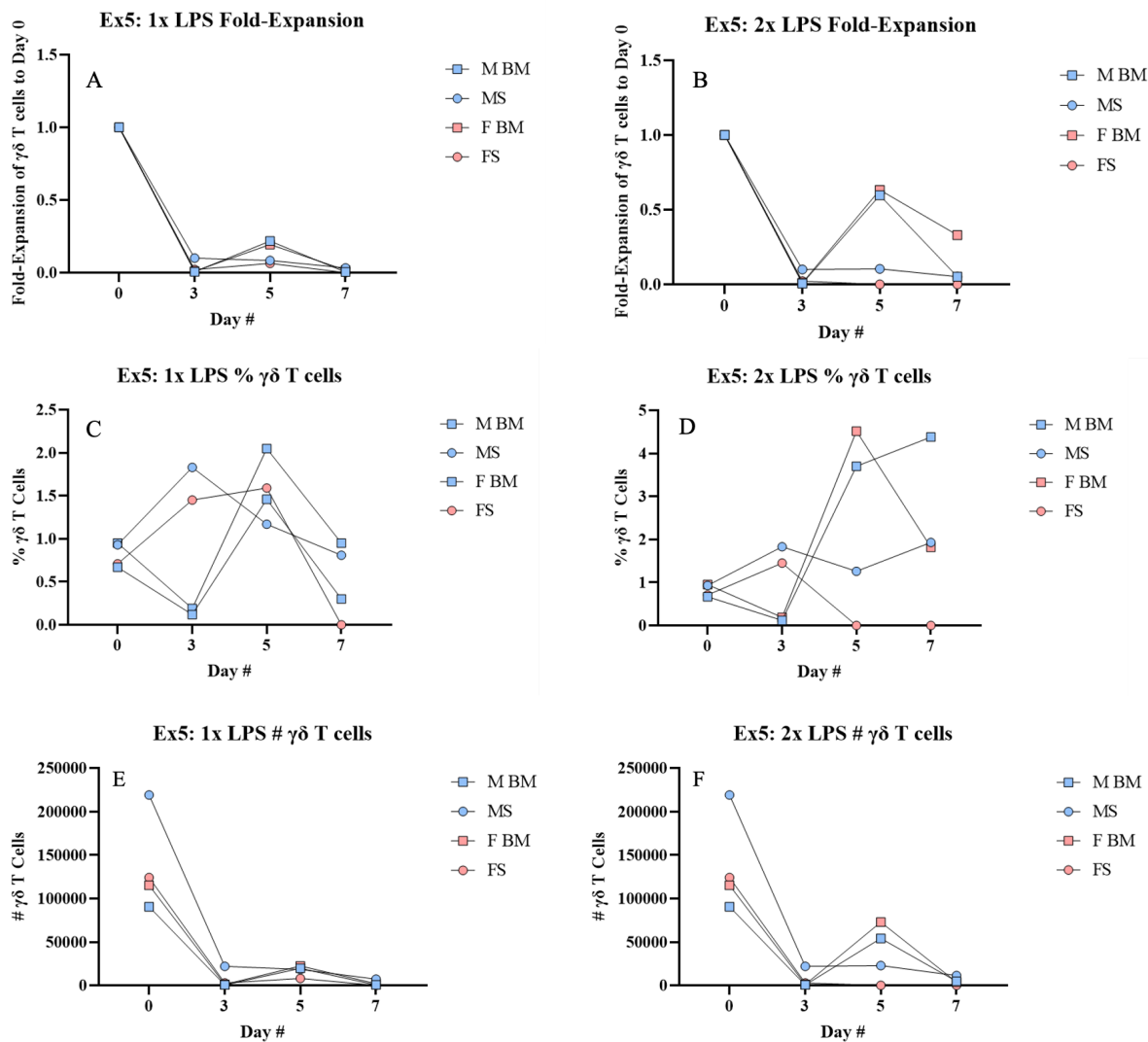


**Figure 11.** This graph shows the experimental results throughout the attempted expansion of murine  $\gamma\delta$  T cells using LPS either once on day 0 or twice on both day 0 and day 3 for experiment 5. Graphs A and B measure the fold-expansion, graphs C and D measure the percentage of  $\gamma\delta$  T cells, and graphs E and F measure the number of gamma delta T cells.

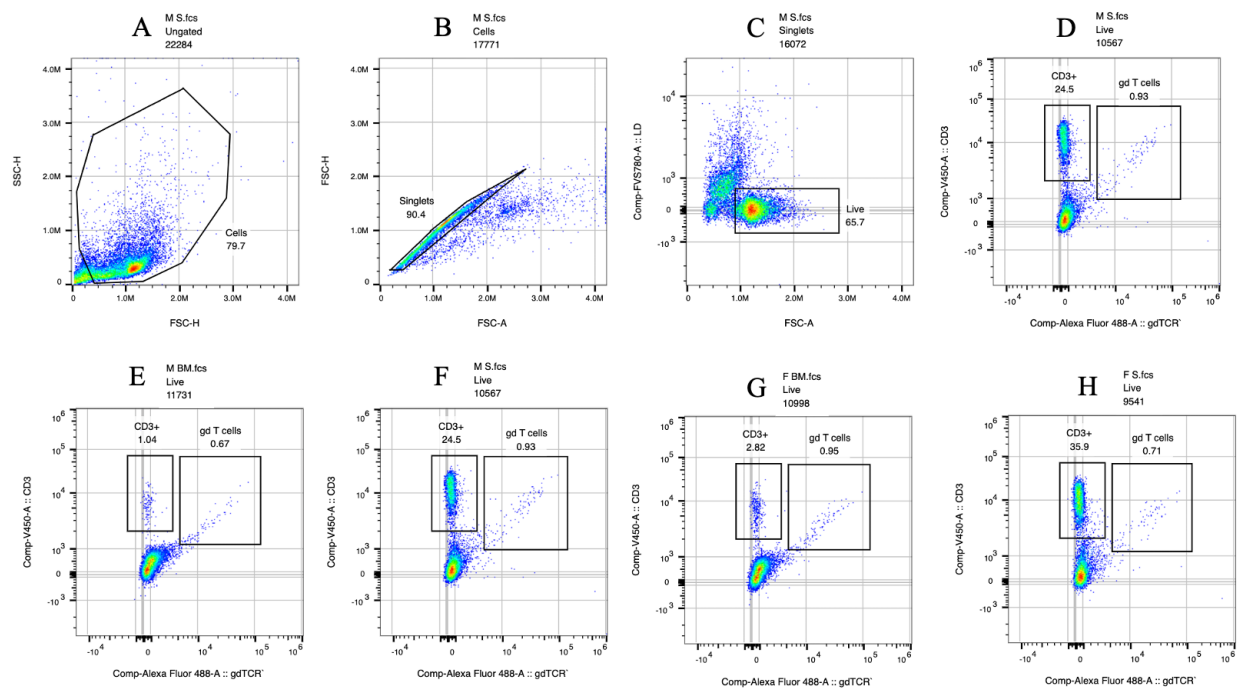


**Figure 12.** This graph shows experiment 5's flow cytometry analysis on day 0 of the attempt at murine  $\gamma\delta$  T cell expansion using LPS. Figures A-D shows the gating strategy for the male spleen. Figures E through H show the percentage of murine CD3+ and  $\gamma\delta$  T cells. This flow demonstrates an example of murine  $\gamma\delta$  T cells before depletion.

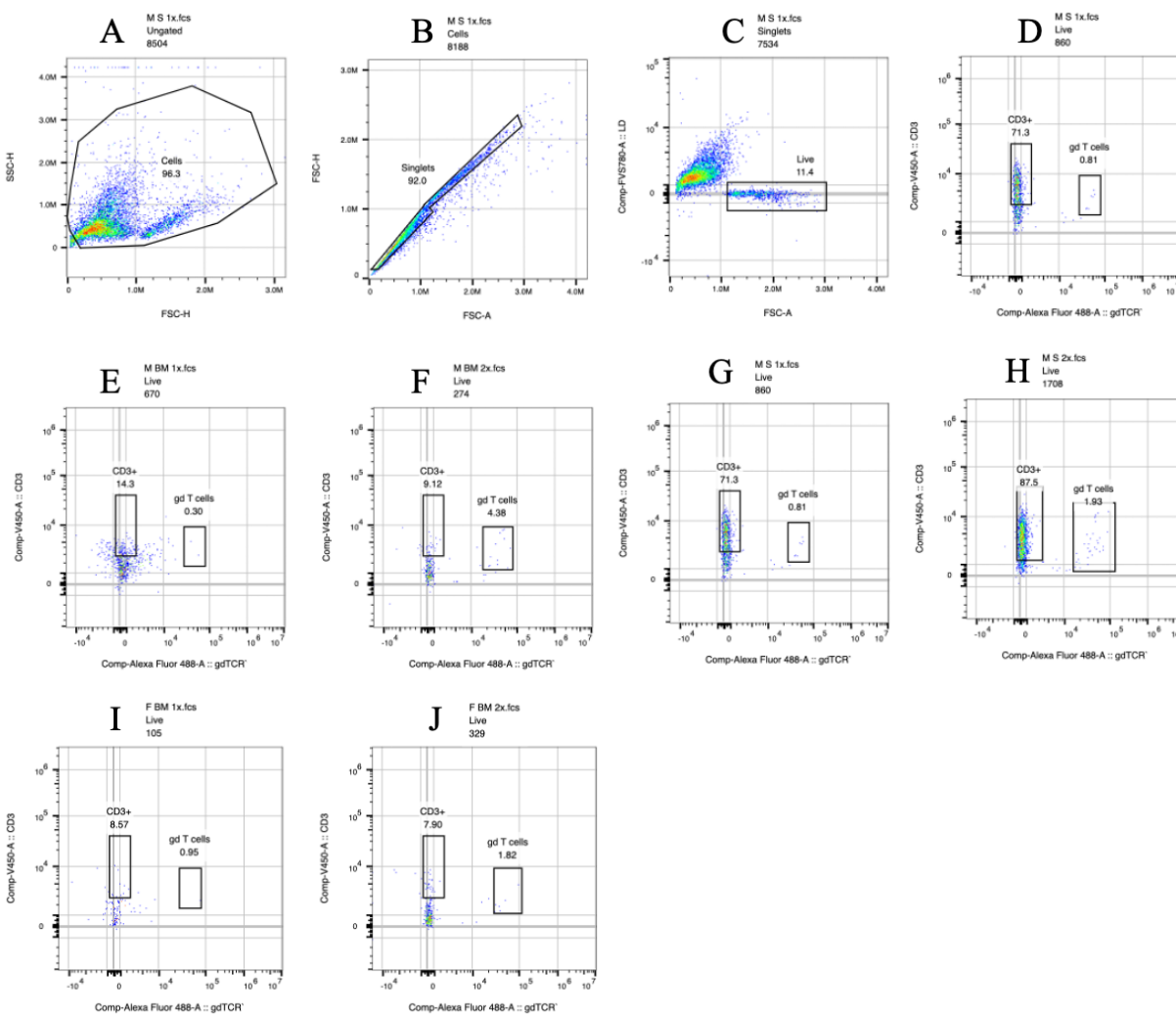


**Figure 13.** This graph shows the flow cytometry analysis of experiment 5's day 7 attempt at murine  $\gamma\delta$  T cell expansion using LPS. Graphs A-D show the gating strategy for the male spleen. Figures E-J show the percentages of CD3+ T cells and murine  $\gamma\delta$  T cells.

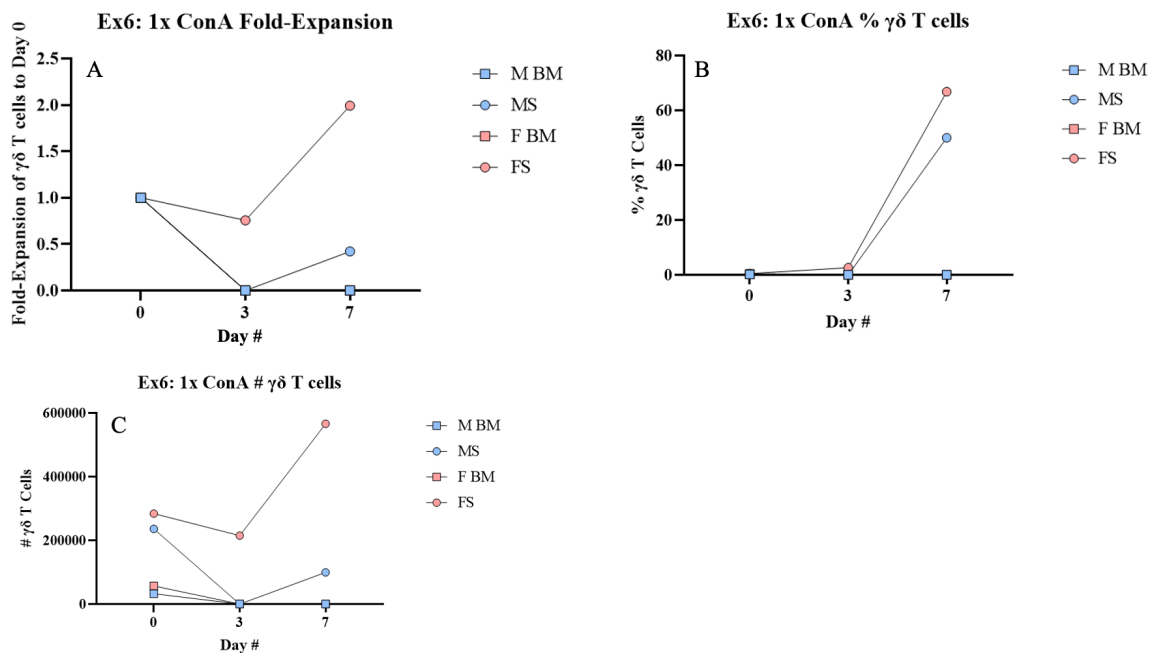


**Figure 14.** This graph shows the timeline of experiment 6's attempted expansion of murine  $\gamma\delta$  T cells using ConA once on Day 0. Graph A describes the fold-expansion, Graph B describes the percentage of  $\gamma\delta$  T cells and Graph C describes the number of  $\gamma\delta$  T cells.

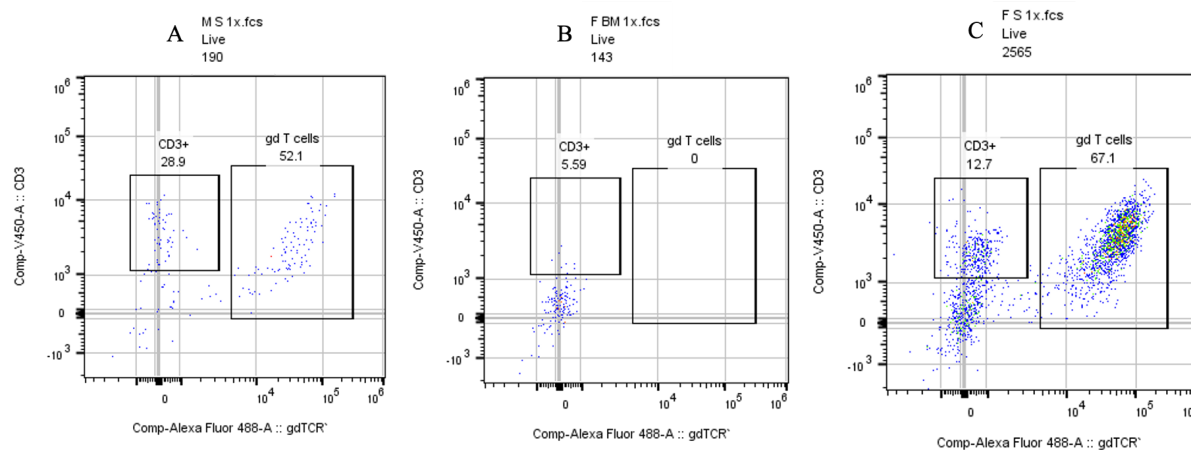


**Figure 15.** This graph shows the flow cytometry analysis of experiment 6's day 7 attempt at murine  $\gamma\delta$  T cell expansion using ConA. There is no flow cytometry data on the percentage of  $\gamma\delta$  T cells for male bone marrow because they had died out. Graph A shows the male spleen, Graph B shows the female bone marrow, and Graph C shows the female spleen. Each graph shows the percentage of CD3+ cells and  $\gamma\delta$  T cells in the culture.

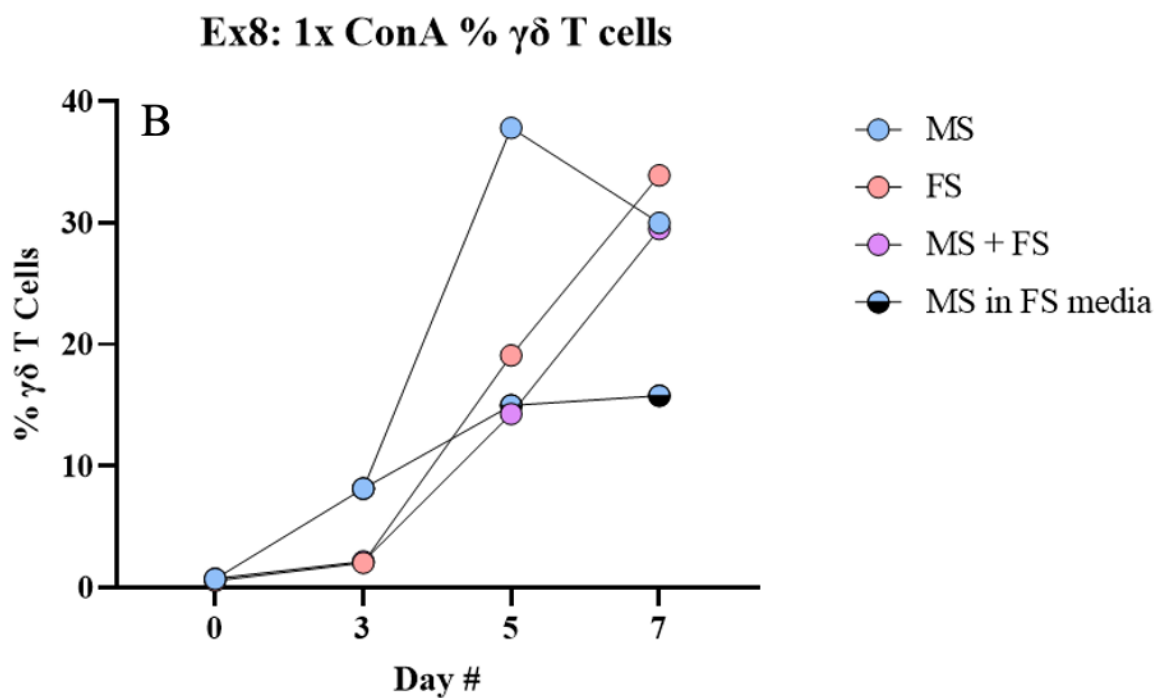
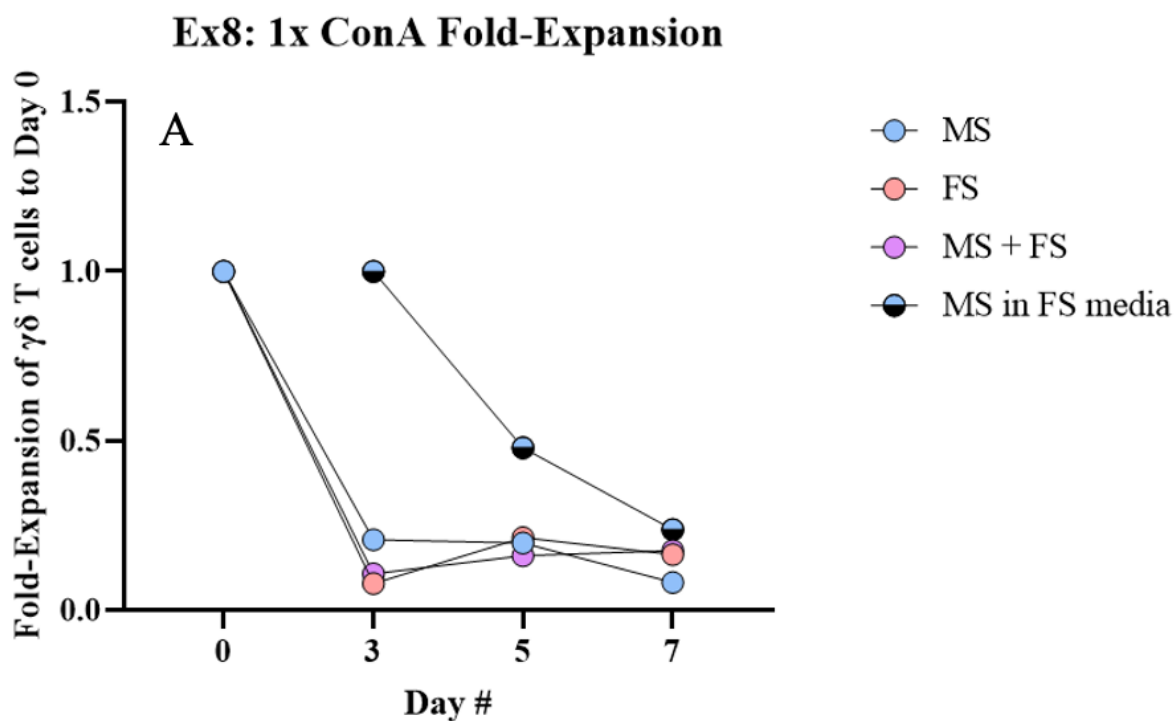


**Figure 16.** This graph shows the timeline of experiment 8's attempted expansion of murine  $\gamma\delta$  T cells using ConA once on day 0. Graph A shows the fold-expansion while Graph B shows the percentage of  $\gamma\delta$  T cells.



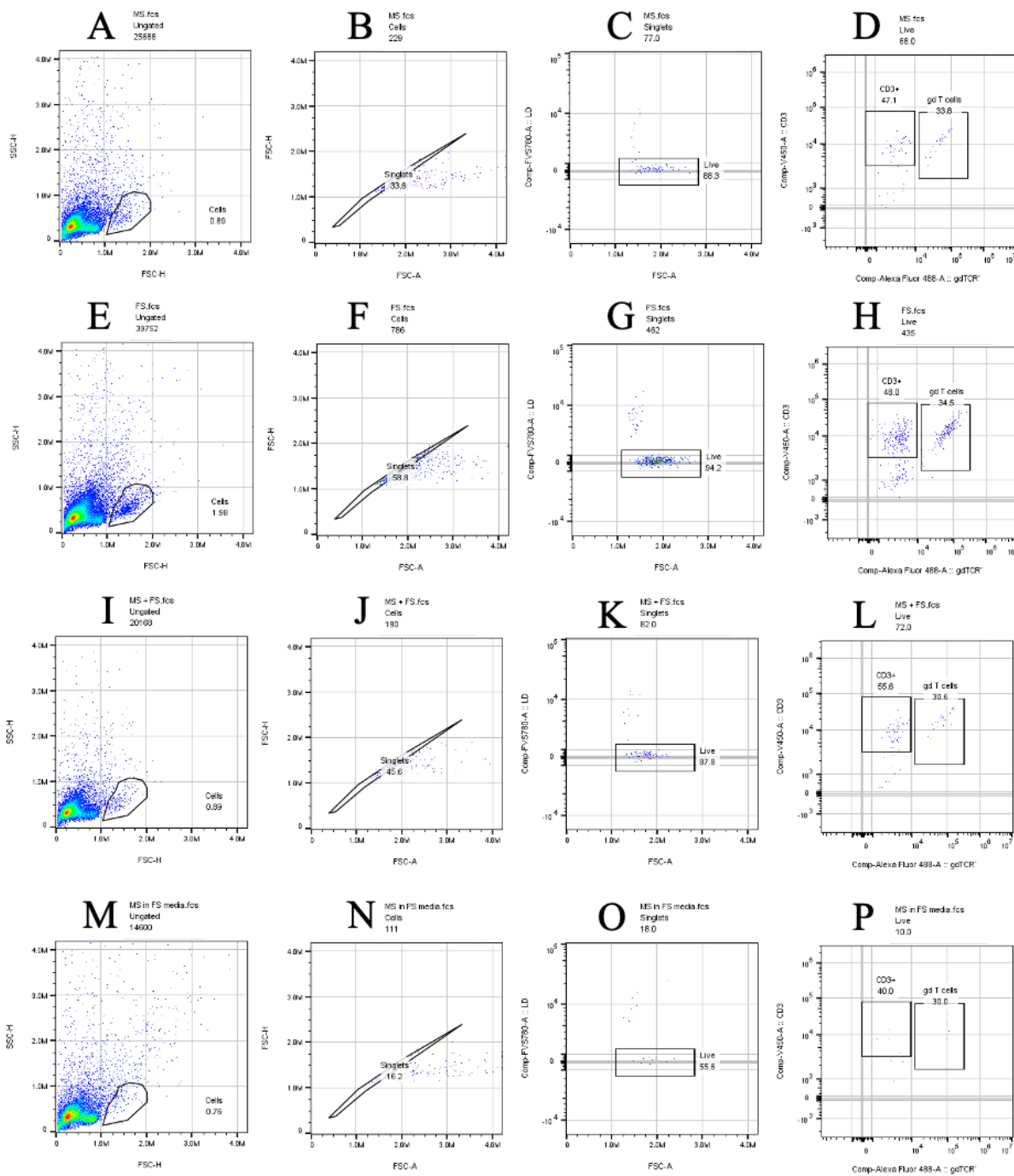


**Figure 17.** This graph shows the flow cytometry analysis of experiment 8's day 7 attempted murine  $\gamma\delta$  T cell expansion using ConA. The gating strategies for male spleen (A-D), female spleen (E-H), male and female spleen combined (I-L), and male spleen in female media (M-P) are shown above.

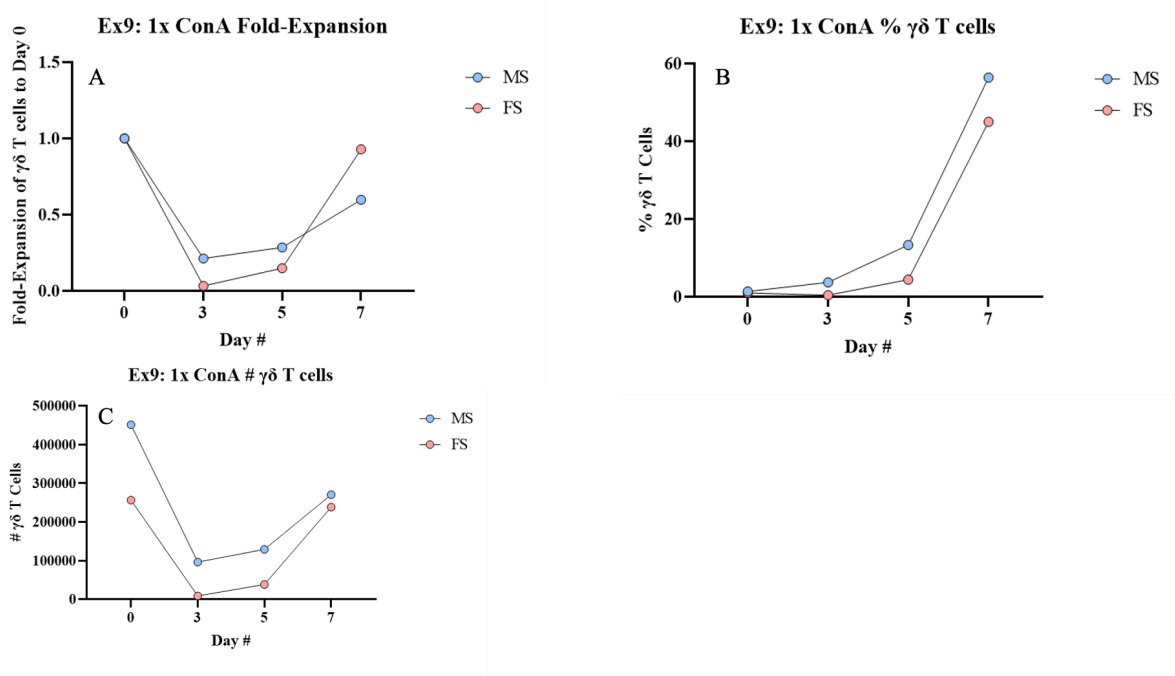


**Figure 18.** This graph shows the timeline of experiment 9’s attempted expansion of murine  $\gamma\delta$  T cells using ConA once on Day 0. Graph A shows the fold-expansion, Graph B shows the percentage of  $\gamma\delta$  T cells, and Graph C shows the number of  $\gamma\delta$  T cells.

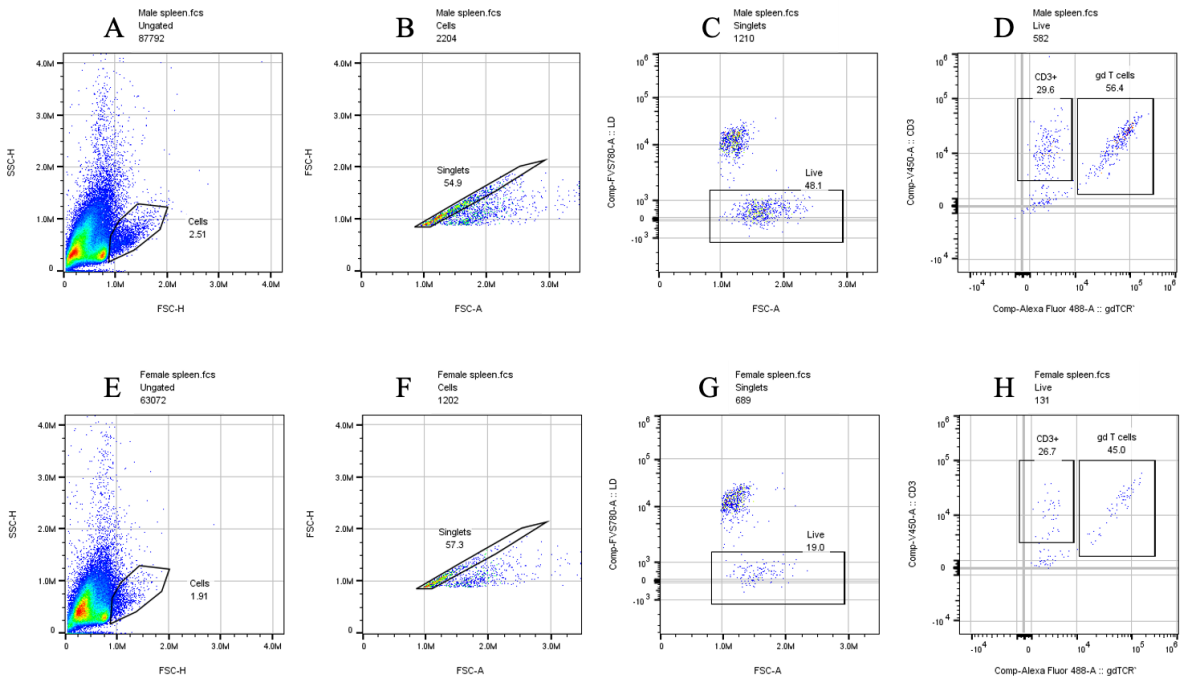


**Figure 19.** This figure shows the flow cytometry analysis of experiment 9's day 7 attempt at expanding murine  $\gamma\delta$  T cells using ConA. The following graphs show the gating scheme for male spleen (A-D) and female spleen (E-H).

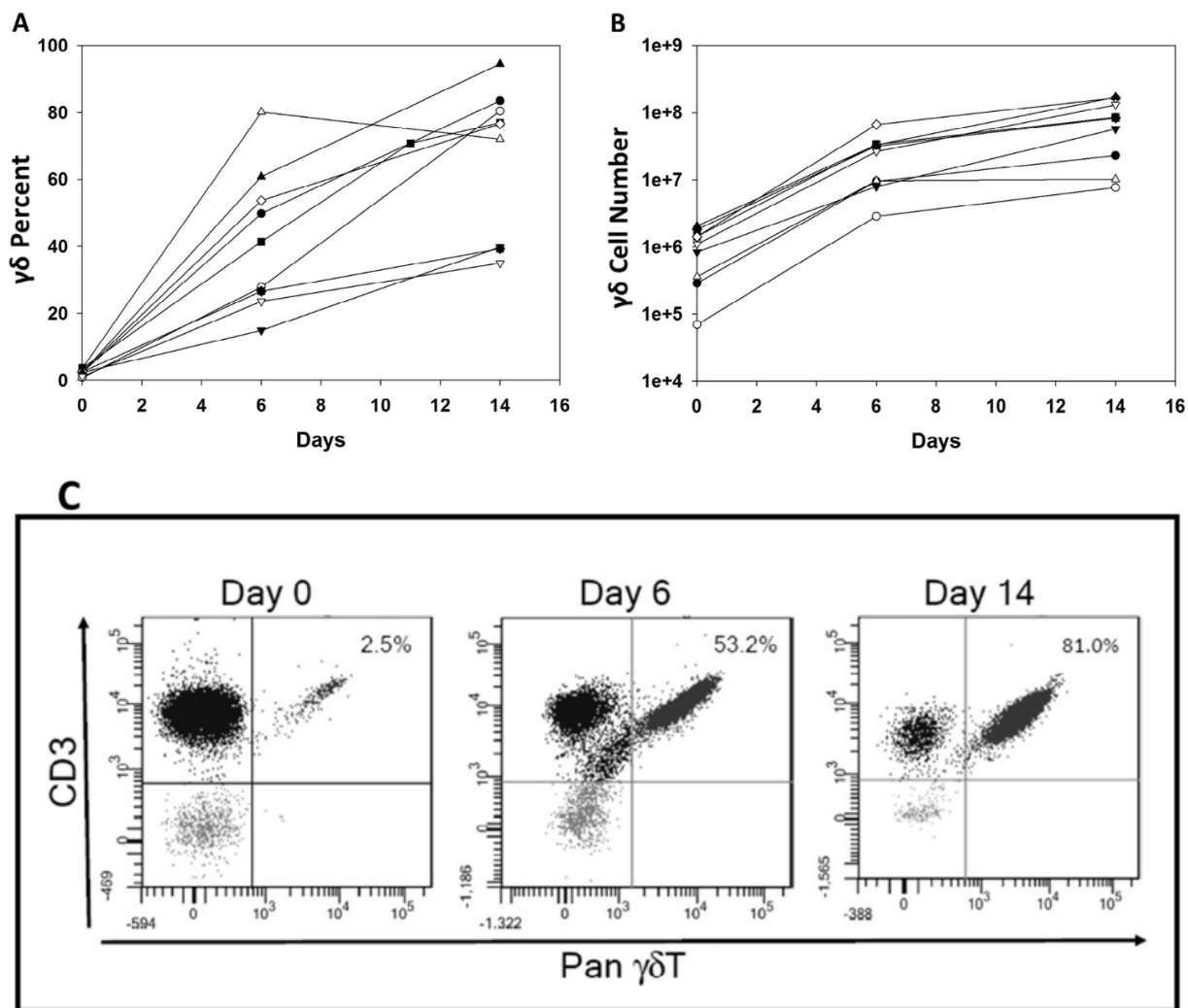


**Figure 20.** This figure and the corresponding text show an example of what kind of human  $\gamma\delta$  T cell expanding ability that our lab has been able to achieve from various donors. Graph A shows an example of how the percentage of human  $\gamma\delta$  T cells changes over the two week expansion protocol, Graph B shows how the number of murine  $\gamma\delta$  T cells increases over the expansion protocol, and Graph C shows how the flow looks after the expansion protocol, including the presence of CD3<sup>+</sup> T cells (Sutton et al. 2016).

## $\gamma\delta$ Expansion Protocol

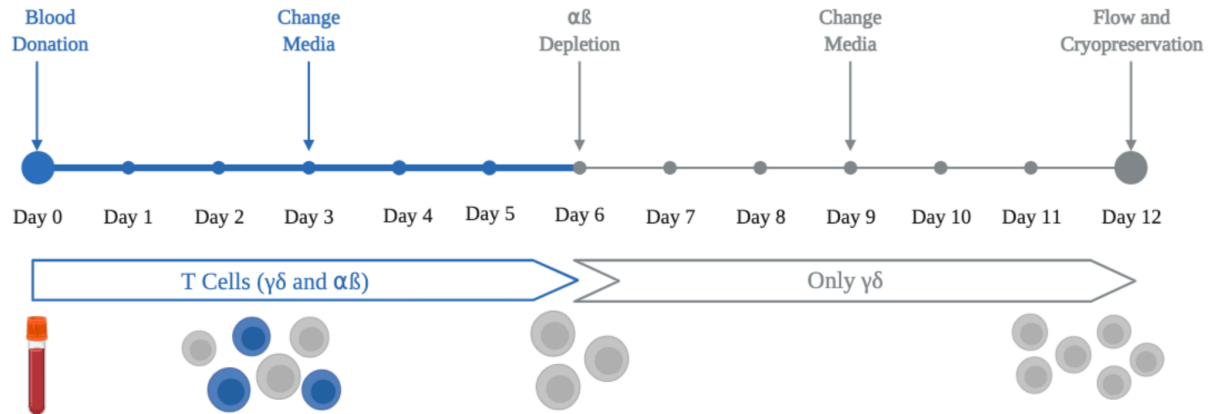


**Figure 21.** This figure details the major steps needed to expand human  $\gamma\delta$  T cells from the blood. A sample from a donor is collected on Day 0, where PBMCs (containing T cells) are cultured. On day 3, the products are recultured before day 6, where an  $\alpha\beta$  depletion occurs. This means that the remainder of the expansion deals only with  $\gamma\delta$  T cells. On day 9, the cells are recultured and on day 12, the  $\gamma\delta$  T cells are cryopreserved. Taken from a presentation done by our lab (Ung, Branella, and Spencer 2022). Created with BioRender.com.

# Electroporation Protocol

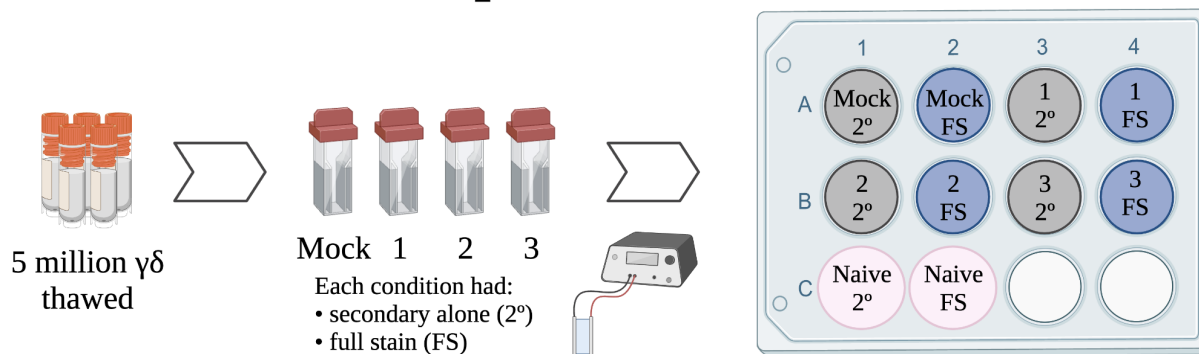


**Figure 22.** This figure details the major steps needed in order to electroporate human  $\gamma\delta$  T cells that were cryopreserved. On day 0, 5 tubes of 5 million human  $\gamma\delta$  T cells were thawed and electroporated with an SCF CAR. After electroporation, the cells were cultured. The next day they were analyzed with flow cytometry. Modified from a presentation from our lab (Ung, Branella, and Spencer 2022). Created with BioRender.com.

Electric Field (V/cm)	Voltage (V)	Time of electroporation (ms)	Cuvette Gap (mm)	Brand	Mock or SCF
1250	500	5	4	Fisher	Mock
1250	500	5	4	Fisher	SCF
1000	200	2	2	Biorad	Mock
1000	200	2	2	Biorad	SCF
1250	500	2	4	Biorad	Mock
1250	500	2	4	Biorad	SCF

**Table 2.** This table describes the various parameters used to manipulate this experiment for the transfection of human  $\gamma\delta$  T cells. Data used for another presentation from our lab (Ung, Branella, and Spencer 2022).

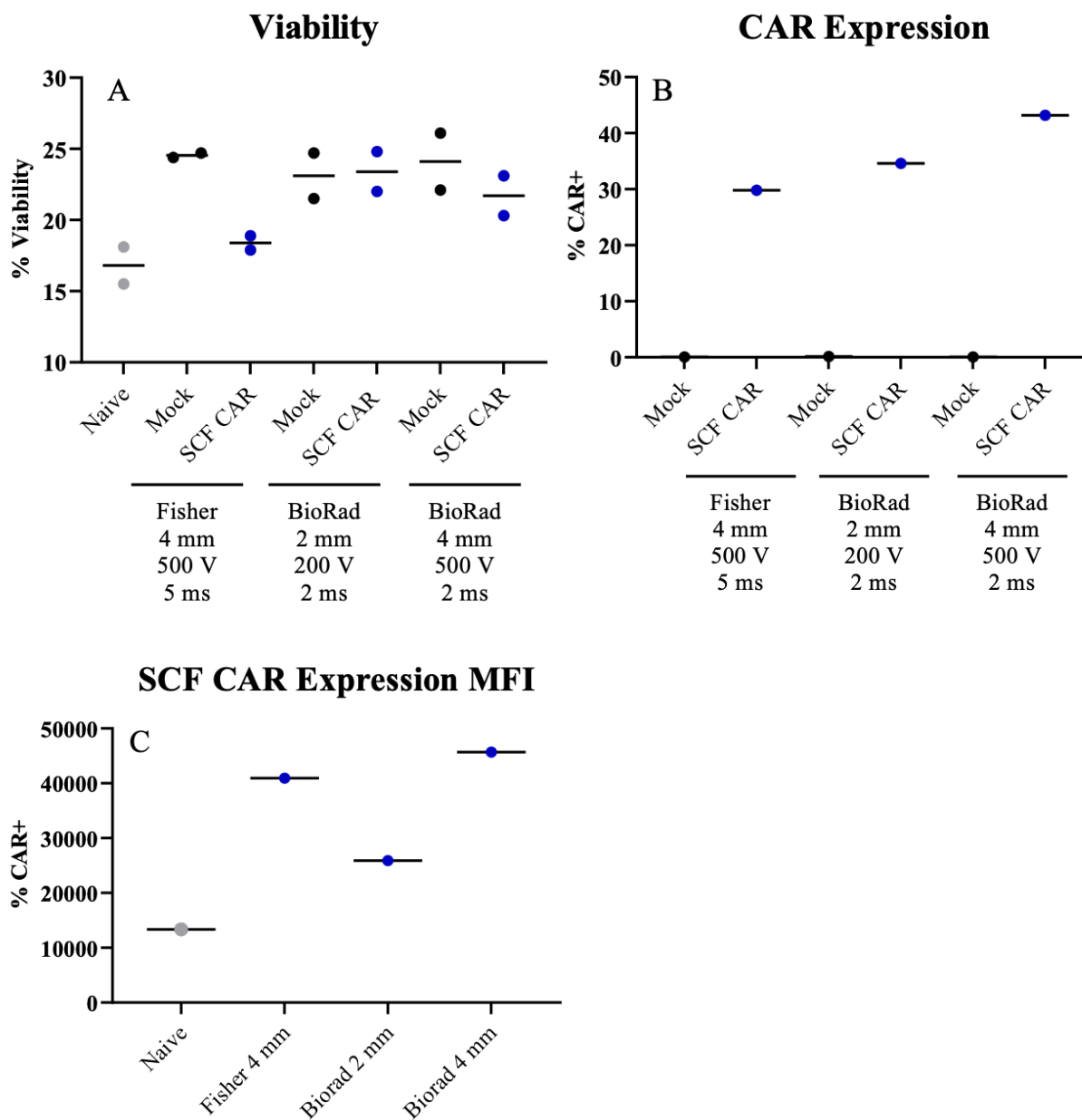


**Figure 23.** These figures are used to evaluate the success of the human  $\gamma\delta$  CAR T cell transfection protocol. Graph A demonstrates the viability of the cells post-electroporation (with the exception of the naive cells), Graph B demonstrates the %CAR+ cells post-transfection, and Graph C demonstrates the MFI for each condition. Modified from a presentation from our lab (Ung, Branella, and Spencer 2022).